© 2022. Published by The Company of Biologists Ltd | Development (2022) 149, dev200767. doi:10.1242/dev.200767

RESEARCH ARTICLE

Mesenchymal FGFR1 and FGFR2 control patterning of the ureteric mesenchyme by balancing SHH and BMP4 signaling

Lena Deuper[1], Max Meuser[1], Hauke Thiesler[2], Ulrich W. H. Jany[1], Carsten Rudat[1], Herbert Hildebrandt[2], Mark-Oliver Trowe[1] and Andreas Kispert[1,*]

ABSTRACT

The coordinated development of the mesenchymal and epithelial progenitors of the murine ureter depends on a complex interplay of diverse signaling activities. We have recently shown that epithelial FGFR2 signaling regulates stratification and differentiation of the epithelial compartment by enhancing epithelial *Shh* expression, and mesenchymal SHH and BMP4 activity. Here, we show that FGFR1 and FGFR2 expression in the mesenchymal primordium impinges on the SHH/BMP4 signaling axis to regulate mesenchymal patterning and differentiation. Mouse embryos with conditional loss of *Fgfr1* and *Fgfr2* in the ureteric mesenchyme exhibited reduced mesenchymal proliferation and prematurely activated lamina propria formation at the expense of the smooth muscle cell program. They also manifested hydroureter at birth. Molecular profiling detected increased SHH, WNT and retinoic acid signaling, whereas BMP4 signaling in the mesenchyme was reduced. Pharmacological activation of SHH signaling in combination with inhibition of BMP4 signaling recapitulated the cellular changes in explant cultures of wild-type ureters. Additional experiments suggest that mesenchymal FGFR1 and FGFR2 act as a sink for FGF ligands to dampen activation of *Shh* and BMP receptor gene expression by epithelial FGFR2 signaling.

KEY WORDS: FGF, Patterning, Smooth muscle cells, Ureter, Lamina propria, SHH, BMP4

INTRODUCTION

The ureters are a pair of straight tubes that account by means of peristaltic contractions for the active transport of urine from the renal pelvises to the bladder. The structural basis for this activity is an outer mesenchymal tissue compartment with a three-layered organization of fibroelastic material on the inside (the lamina propria) and outside (the tunica adventitia), and contractile smooth muscle cells (SMCs) in the middle (the tunica muscularis) (Velardo, 1981). This ordered arrangement of fibrocytes and SMCs is the result of a complex interplay of proliferation, patterning and differentiation processes that occurs in the common progenitor pool of these cell types. In the mouse, ureteric mesenchyme (UM) progenitors are first recognized around embryonic day (E) 11.0 as a homogenous population of *Tbx18*$^{+}$ mesenchymal cells. These cells surround the distal aspect of the epithelial ureteric bud, the primordium of the specialized three-layered inner epithelial lining of the ureter, the urothelium (Bohnenpoll et al., 2013). The mesenchymal cells directly adjacent to the ureteric epithelium (UE) acquire at E12.5 a rhomboid shape, express at E14.5 *Myocd*, the master regulator of SMC differentiation (Wang et al., 2001; Wang and Olson, 2004), and activate until birth a cascade of SMC structural genes. Notably, from E14.5 to E16.5 some of these cells switch off *Myocd* expression, populate the region between the committed SMCs and the UE, multiply and start to produce abundant extracellular matrix to form the lamina propria. The cells in the outer layer of the UM retain their loose organization and differentiate from E13.5 onwards into adventitial fibrocytes (Bohnenpoll et al., 2017a).

Proliferation, patterning and SMC differentiation of the UM depends on signals from the adjacent UE (Baskin et al., 1996; Bohnenpoll and Kispert, 2014; Cunha, 1976), of which SHH and WNTs have been characterized as essential. *Shh* is expressed from E11.5 to E14.5 in the UE and activates SMO-dependent signaling in the adjacent UM to assure survival in the outer region, and proliferation and SMC differentiation in the inner region. The latter functions are mediated by the transcription factor FOXF1 and the signaling molecule BMP4 (Bohnenpoll et al., 2017c; Yu et al., 2002). BMP4 also acts *in trans* to activate proliferation, stratification and differentiation of the UE (Mamo et al., 2017). Epithelial WNTs suppress the outer adventitial fate and foster SMC differentiation, at least partly through induction of the transcriptional repressors TBX2 and TBX3 (Aydoğdu et al., 2018; Trowe et al., 2012). SMC differentiation is negatively impacted by retinoic acid (RA), which is produced by ALDH1A2 in the UM and by ALDH1A1 and ALDH1A3 in the UE (Bohnenpoll et al., 2017b). How these signaling pathways are temporally and spatially regulated and integrated to activate *Myocd* and the SMC program in the inner layer of the UM precisely at E14.5 is not known but feed-forward and feed-back mechanisms are central (Meuser et al., 2022; Weiss et al., 2019). Insight into this regulatory network is important because defects in SMC differentiation present a relevant subgroup of human congenital anomalies of the kidney and the urinary tract (Capone et al., 2017).

Fibroblast growth factors (FGFs) are a family of more than 20 secreted proteins that bind with high affinity to at least four members of a family of receptor tyrosine kinases, termed FGFR1-FGFR4. Ligand-receptor interaction activates downstream modules to trigger changes of cell behavior in a variety of biological contexts in both a transcriptionally dependent and independent manner (Laestander and Engström, 2014; Ornitz and Itoh, 2015). Signaling through FGFR1 and FGFR2 has been implicated in the development of numerous tissues and organs, including those of the excretory system (Walker et al., 2016). We have recently shown that *Fgf7* and *Fgf10* are expressed in the UM from E11.5 to E14.5.

[1]Institute of Molecular Biology, Medizinische Hochschule Hannover, 30625 Hannover, Germany. [2]Institute of Clinical Biochemistry, Medizinische Hochschule Hannover, 30625 Hannover, Germany.

*Author for correspondence (kispert.andreas@mh-hannover.de)

M.M., 0000-0001-9621-1889; U.W.H.J., 0000-0003-4506-3817; C.R., 0000-0002-8877-7767; H.H., 0000-0002-1044-0881; M.-O.T., 0000-0002-0011-461X; A.K., 0000-0002-8154-0257

Handling Editor: Liz Robertson
Received 18 March 2022; Accepted 19 August 2022

Development (2022) 149, dev200767. doi:10.1242/dev.200767

Fgfr1 and *Fgfr2* which encode the cognate receptors for these ligands (Igarashi et al., 1998; Jans, 1994), are expressed in the UE at these stages (Meuser et al., 2022). Conditional deletion of *Fgfr2* in the UE resulted in a defect in urothelial stratification and lack of intermediate and basal cell differentiation as well as in delayed SMC and lamina propria differentiation due to a reduction of *Shh* expression and SHH/BMP4 signaling (Meuser et al., 2022). *Fgfr1* and *Fgfr2* are also expressed in the UM at E12.5 and E14.5 (Meuser et al., 2022), indicating a functional relevance for the development of this tissue. Defects in mesenchymal patterning and SMC differentiation in bladders that specifically lack *Fgfr2* in the mesenchymal compartment support this notion (Ikeda et al., 2017).

Here, we used a conditional gene targeting strategy to analyze *Fgfr1* and *Fgfr2* function in the mouse UM. We show that *Fgfr1* and *Fgfr2* maintain the structural and functional integrity of the ureter by patterning the mesenchymal tissue. We provide evidence that mesenchymal FGFR1 and FGFR2 balance SHH and BMP4 signaling by limiting the activation of epithelial FGFR2 signaling.

RESULTS

Loss of *Fgfr1* and *Fgfr2* in the UM leads to hydroureter formation at birth

Fgfr1 and *Fgfr2* are expressed in the epithelial and mesenchymal compartment of the developing ureter at E12.5 and (very weakly) at E14.5 (Fig. S1A). To investigate the mesenchymal function of *Fgfr1* and *Fgfr2* in this organ rudiment, we used a conditional gene inactivation approach with floxed alleles of *Fgfr1* and *Fgfr2* (Hoch and Soriano, 2006; Yu et al., 2003), and a *Tbx18*^{cre} line that mediates recombination in the UM starting from E10.5 (Airik et al., 2010; Bohnenpoll et al., 2013).

Matings of *Tbx18*$^{cre/+}$;*Fgfr1*$^{fl/+}$;*Fgfr2*$^{fl/+}$ males with *Fgfr1*$^{fl/fl}$;*Fgfr2*$^{fl/fl}$ females gave rise to offspring with a normal distribution of all mutant genotypes and with a normal external appearance at all embryonic stages analyzed (Table S1). Morphological inspection of preparations of whole urogenital systems at E18.5, however, revealed hydroureter in 50% of *Tbx18*$^{cre/+}$;*Fgfr1*$^{fl/+}$;*Fgfr2*$^{fl/+}$, in 64% of *Tbx18*$^{cre/+}$;*Fgfr1*$^{fl/fl}$;*Fgfr2*$^{fl/+}$ and in 100% of the mutants with complete loss of *Fgfr2* function (*Tbx18*$^{cre/+}$;*Fgfr1*$^{fl/+}$;*Fgfr2*$^{fl/fl}$, *Tbx18*$^{cre/+}$;*Fgfr1*$^{fl/fl}$;*Fgfr2*$^{fl/fl}$). In the latter two combinations, a shift from mild to strong hydroureter was observed in approximately 20% of the cases (Table S2, Fig. S2, Fig. 1A). This argues for an additive contribution of mutant *Fgfr1* and *Fgfr2* alleles to the observed phenotype with *Fgfr2* being more important. In mutants with complete loss of *Fgfr2* function, the adrenals were drastically reduced in size (Fig. 1A, Fig. S2). We have recently shown that this phenotype relates to a function of *Fgfr2* in expansion of adrenogonadal progenitors in which *Tbx18*^{cre} also mediates recombination (Hafner et al., 2015).

Given the more robust and severe phenotype of mutants with complete loss of *Fgfr1* and *Fgfr2* function, we concentrated on *Tbx18*$^{cre/+}$;*Fgfr1*$^{fl/fl}$;*Fgfr2*$^{fl/fl}$ (*Fgfr1/2cDKO-UM*) embryos for further analysis. Littermates without the *Tbx18*^{cre} allele were used as controls. Histological inspection of the urogenital system of *Fgfr1/2cDKO-UM* embryos confirmed the presence of a dilated ureter, which at this stage, however, did not translate into hydronephrotic lesions, i.e. dilatation of the renal pelvis and the renal collecting duct system (Fig. 1B). Ureter dilatation can be caused by physical obstruction along the ureter and/or its junction with the bladder or by functional insufficiency of the peristaltic activity of the mesenchymal wall. To interrogate the first option, we injected ink into the renal pelvis. We observed in all mutants, as in the control, a smooth flow of the ink into the bladder (Fig. 1C). Moreover, histological analysis showed a normal insertion of the distal ureter into the dorsal bladder wall (Fig. 1D, arrows). To test for functional insufficiency, we analyzed proximal ureter sections of E18.5 *Fgfr1/2cDKO-UM* embryos for the presence of SMCs. Considering the dilatation of the ureter, markers of this differentiated cell type appeared either unchanged (ACTA2, TAGLN, *Myocd*, *Myh11*), or weakly (*Tnnt2*, *Tagln*, *Actg2*) or strongly (*Ckm*) reduced in their expression (Fig. 1E,F). Expression of *Aldh1a2*, a marker for fibrocytes of the inner lamina propria,

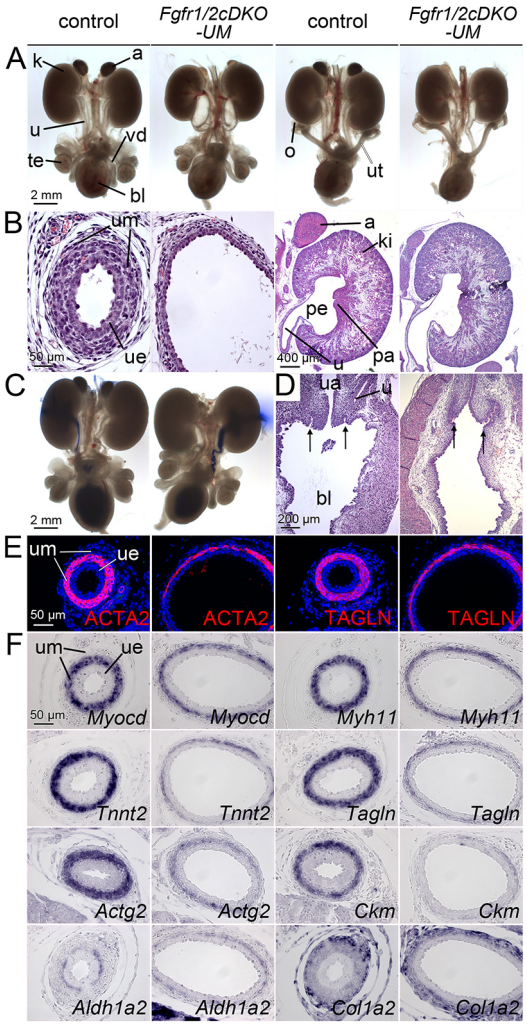

Fig. 1. Ureter anomalies in E18.5 embryos with conditional loss of *Fgfr1* and *Fgfr2* in the UM (*Fgfr1/2cDKO-UM*). (A) Morphology of whole urogenital systems of male (column 1, control: *n*=18; column 2, mutant: *n*=5) and female (column 3, control: *n*=13; column 4, mutant: *n*=4) embryos. (B) Hematoxylin and Eosin staining of transverse sections of the proximal ureter (columns 1 and 2) and of sagittal kidney sections (columns 3 and 4). *n*=3 for all genotypes. (C,D) Analysis of the vesico-ureteric junction by ink injection (control: *n*=8; mutant: *n*=6) (C) and by Hematoxylin and Eosin staining of sagittal bladder sections (control: *n*=3; mutant: *n*=3) (D). Arrows in D indicate the openings of the ureters into the bladder. (E) Immunofluorescence analysis of expression of the SMC proteins ACTA2 and TAGLN on transverse sections of the proximal ureter. Nuclei are counterstained (in blue) with DAPI. (F) Analysis of the expression of markers of SMCs (*Myocd*, *Myh11*, *Tnnt2*, *Tagln*, *Actg2*, *Ckm*), the lamina propria (*Aldh1a2*) and the tunica adventitia (*Col1a2*) by RNA *in situ* hybridization on transverse sections of the proximal ureter. *n*≥3 for all probes and genotypes in D,E. a, adrenal; bl, bladder; k/ki, kidney; o, ovary; pa, papilla; pe, pelvis; te, testis; u, ureter; ua, urethra; ue, ureteric epithelium; um, ureteric mesenchyme; ut, uterus; vd, vas deferens.

Development (2022) 149, dev200767. doi:10.1242/dev.200767

appeared increased in the mutant, whereas *Col1a2*, a marker for outer adventitial fibrocytes, was unchanged (Fig. 1F), again taking the ureter dilatation into account.

Urothelial differentiation was unaffected as revealed by normal expression of KRT5, ΔNP63 and UPK1B, which combinatorially mark basal cells ($KRT5^{+}\Delta NP63^{+}UPK1B^{-}$), intermediate cells ($KRT5^{-}\Delta NP63^{+}UPK1B^{+}$) and superficial cells ($KRT5^{-}\Delta NP63^{-}UPK1B^{+}$) (Bohnenpoll et al., 2017a) (Fig. S3). Together, this argues for defects in SMC differentiation as cause of hydroureter in *Fgfr1/2cDKO-UM* embryos.

Fgfr1/2cDKO-UM ureters exhibit a delay in SMC differentiation and premature lamina propria formation

To define the onset as well as the progression of the mesenchymal differentiation defects, we performed marker analysis at earlier stages of ureter development (Fig. 2). In the control, *Myocd* was strongly activated in the inner layer of the UM at E14.5. *Myh11*, *Tagln*, *Actg2*, ACTA2 and TAGLN followed at E15.5; *Tnnt2* and *Ckm* at E16.5. In *Fgfr1/2cDKO-UM* ureters, all of these markers were very weakly activated at the respective time points and/or were strongly reduced when dilatation occurred at E16.5. *Aldh1a2* was weakly expressed in the entire UM in the control at E14.5 but vanished subsequently. In the mutant, strong expression of *Aldh1a2* was found in the inner layer of the UM from E14.5 to E16.5 (Fig. 2A, arrows). Expression of *Col1a2* was unchanged. Epithelial differentiation was unaffected as indicated by normal activation of ΔNP63 at E14.5, of UPK1B at E15.5 and of KRT5 in few cells of the basal layer of the UE at E16.5 (Fig. S4).

Histological staining detected a normal subdivision of the mutant UM into an inner condensed and an outer loosely organized layer at E12.5 and E14.5 (Fig. S5A). The terminal deoxynucleotidyl transferase dUTP nick end labeling (TUNEL) assay did not expose changes in apoptosis in the UM at either stage (Fig. S5B). In contrast, a 5-bromo-2′-deoxyuridine (BrdU) incorporation assay

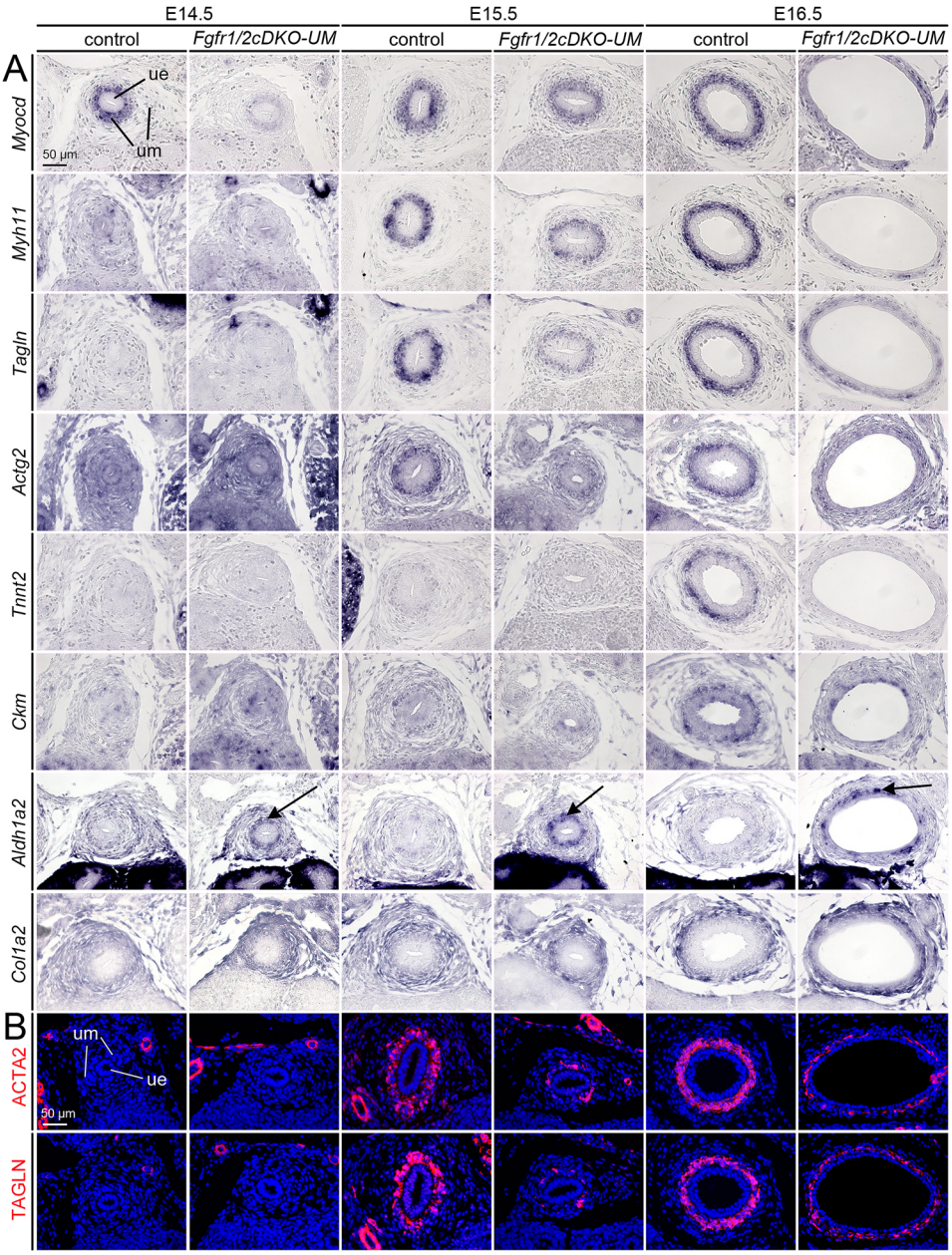

Fig. 2. Early onset of mesenchymal differentiation defects in *Fgfr1/2cDKO-UM* ureters. (A,B) Expression analysis on transverse sections of the proximal ureter region of E14.5, E15.5 and E16.5 embryos for markers of SMCs (*Myocd*, *Myh11*, *Tagln*, *Actg2*, *Tnnt2*, *Ckm*), the lamina propria (*Aldh1a2*) and the tunica adventitia (*Col1a2*) by RNA *in situ* hybridization analysis (A) and for the SMC proteins ACTA2 and TAGLN by immunofluorescence (B). Nuclei are counterstained (in blue) with DAPI in B. Note that *Aldh1a2* is ectopically activated in the inner layer of the UM (arrows). $n \geq 3$ for all probes, genotypes and assays. ue, ureteric epithelium; um, ureteric mesenchyme.

Development (2022) 149, dev200767. doi:10.1242/dev.200767

revealed reduced proliferation in the inner layer of the UM of mutant embryos at E12.5 (Fig. S5C,D, Table S3). Hence, mesenchymal *Fgfr1* and *Fgfr2* function is required to maintain proliferation in the inner layer of the undifferentiated UM, to suppress lamina propria development and to activate the SMC program in a timely manner.

Delayed onset and compromised progression of peristalsis in *Fgfr1/2cDKO-UM* ureters

As SMC differentiation underlies the peristaltic activity of the ureter, a delayed onset and/or compromised progression of this program may translate into delayed or altered ureter contractions. We tested this hypothesis, by explanting ureters at E13.5 and scoring for peristaltic activity during 8 days of culture (Fig. 3). Wild-type ureters initiated contractions at day 3 of the culture and increased in frequency to 3.5 contractions per minute until day 8 (Fig. 3A,B). Mutant ureters started contractions at day 4 or 5 in culture (Fig. 3A, Table S4A); the contraction frequency was reduced by 50% at day 5 and by 20% at day 8 (Fig. 3B, Table S4B). The contraction intensity was markedly diminished throughout the culture period (Fig. 3C, Table S4C).

Fgfr1/2cDKO-UM ureters explanted at E15.5 behaved similarly. Onset of peristaltic activity was delayed by 2 days, and contraction frequency and intensity were reduced but approached the level of the control at the end of the culture period after 6 days (Fig. S6, Table S5). To investigate whether the SMC phenotype is still compromised at this endpoint, we performed global analysis of transcriptional changes using microarray technology. Using a fold change of at least 1.5 and an intensity threshold of 100 as additional filter, we identified 189 genes that were consistently upregulated and 201 genes that were downregulated in *Fgfr1/2cDKO-UM* ureters (Tables S6 and S7; GEO submission GSE197368). Functional annotation using the DAVID webtool did not uncover any terms related to 'muscle' or 'contraction' in the list of upregulated genes (Tables S8 and S9), and 'regulation of cardiac muscle contraction' at position 97 only in the list of downregulated genes. Manual inspection identified downregulation of the SMC structural genes *Myh6* (−5.0) and *Ckm* (−4.1; it was not detected owing to an intensity <100 in one of the two pools), whereas other SMC-specific genes (*Actg2*, *Acta2*, *Cnn1*, *Myh11*, *Myocd*, *Pcp4l1*, *Tagln*, *Tnnt2*) were unchanged. Expression analysis confirmed downregulation of *Ckm*; *Myh6* provided only unspecific staining. All other SMC markers were unchanged in 6-day explant cultures of E15.5 *Fgfr1/2cDKO-UM* ureters (Fig. S7). Hence, loss of *Fgfr1 and Fgfr2* in the UM does not abrogate SMC differentiation, but delays and partially compromises it. Contraction frequency and intensity can be largely recovered in *ex vivo* culture conditions in the absence of hydrostatic pressure. Interestingly, we found increased and widened expression of *Aldh1a2*/ALDH1A2 (Fig. S7), indicating an expansion of the lamina propria in *ex vivo* conditions.

Altered signaling activities in the UM of *Fgfr1/2cDKO-UM* embryos

We next performed transcriptional profiling by microarray analysis of E14.5 *Fgfr1/2cDKO-UM* and control ureters to identify molecular changes that may underlie the observed cellular defects. Using an intensity threshold of 100 and fold changes of

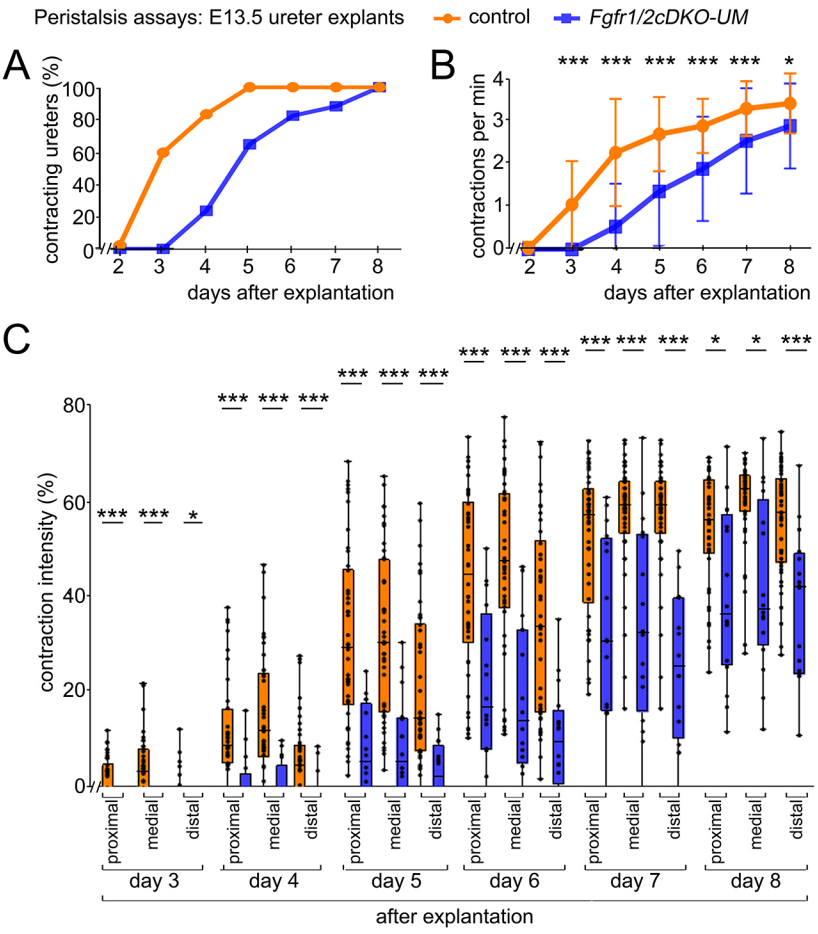

Fig. 3. SMC differentiation and peristaltic activity are delayed but not abrogated in *Fgfr1/2cDKO-UM* ureters. (A-C) E13.5 ureters (control: *n*=42; *Fgfr1/2cDKO-UM*: *n*=17) were explanted and peristaltic activity observed for 8 days in culture. (A) Graph showing the percentage of contracting ureters at any time point of the culture. (B) Graph of the contraction frequency (per min). Values are shown as mean±s.d. (C) Box blot visualizing the contraction intensity. The horizontal line indicates the median. A box contains 50% of all values. Whiskers contain 25% of all values each. Upper and lower whisker borders mark the maximum or minimum value, respectively. **P*<0.05, ****P*<0.001 (two-tailed Student's *t*-test). For detailed values, see Table S4.

Development (2022) 149, dev200767. doi:10.1242/dev.200767

at least 1.25 in the four individual arrays performed, we identified 148 genes that were consistently downregulated and 170 genes that were upregulated in *Fgfr1/2cDKO-UM* ureters (Fig. 4A, Tables S10, S11; GEO submission GSE197369).

Clustering of functional annotation by DAVID did not reveal enriched terms related to relevant molecular pathways in the list of downregulated genes (Table S12). However, manual inspection of the list (Table S10) found strongly decreased expression of the superficial cell marker *Upk1b* (−3.4), as well as of *Grhl3* (−1.6), which encodes a transcription factor essential for superficial cell differentiation (Yu et al., 2009). *In situ* hybridization analysis confirmed reduced expression of these genes as well as of other UPK genes in the UE of E14.5 *Fgfr1/2cDKO-UM* embryos (Fig. S8).

For the list of upregulated genes, functional annotation clustering found terms related to SHH/SMO signaling as the top-enriched, and related to WNT signaling at position 7 (Fig. 4B, Table S13). Manual inspection of this list identified *Shh* and known targets of its activity in the UM (*Foxl1*, *Foxf1*, *Foxf2*, *Hhip*, *Ptch1*, *Ptch2*) as well as *Wnt9b* and direct targets of WNT signaling activity in the UM (*Sp5*,

A

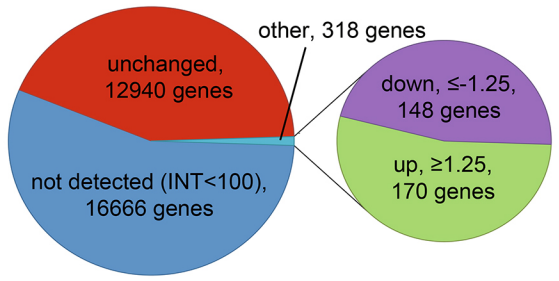

B

Functional annotation clustering for upregulated genes in E14.5 *Fgfr1/2cDKO* ureters

Cluster	Enrichment	Category	Term	P-Value
1	3.22	KEGG_PATHWAY	Hedgehog signaling pathway	3.2E-05
2	2.95	UP_KEYWORDS	Glycoprotein	1.4E-07
3	2.6	INTERPRO	Thrombospondin, type 1 repeat	9.6E-05
4	2.41	GOTERM_CC_DIRECT	proteinaceous extracellular matrix	5.5E-04
5	2.12	GOTERM_BP_DIRECT	cell-cell signaling	1.3E-04
6	2.08	INTERPRO	EGF-like, conserved site	7.2E-05
7	1.94	GOTERM_BP_DIRECT	Wnt signaling pathway	5.5E-03
8	1.89	SMART	EGF	1.7E-03
9	1.84	UP_KEYWORDS	Cell junction	1.7E-03
10	1.75	UP_KEYWORDS	Lipoprotein	6.4E-03

C

Microarray analysis of transcriptional changes in signaling systems in E14.5 *Fgfr1/2cDKO-UM* ureters

relates to	Gene Symbol	FC 1	FC 2	FC 3	FC 4	averageFC
SHH signaling	*Foxl1*	2.1	2.1	1.6	1.9	1.9
	Foxf1	1.5	2.1	1	1.6	1.6
	Ptch1	1.6	1.4	1.5	1.4	1.5
	Ptch2	1.5	1.5	1.4	1.4	1.4
	Hhip	1.6	1.3	1.4	1.8	1.5
	Shh	3.2	1.3	1.5	1.3	1.8
WNT signaling	*Axin2*	2.1	1.7	1.5	1.7	1.8
	Sp5	4.5	5.2	2.3	2.9	3.8
	Wnt7b	1	1.5	1	1.2	1.2
	Wnt9b	2.4	2.6	1.6	1.4	2
RA signaling	*Aldh1a1*	2	2	1.6	1.2	1.7
	Aldh1a2	1.4	1.4	1.4	1.1	1.3
	Aldh1a3	4.7	5.7	3.3	4.1	4.5
	Cyp26a1	1.8	1.9	1.9	2.3	2
	Ecm1	1.3	1.7	1.3	1.8	1.5
	Elf5	1.6	1.6	1.5	1.6	1.6
BMP4 signaling	*Bmp4*	1.2	1.1	1.1	1.3	1.2
	Id2	1	-1.2	1.1	1	1
	Id4	1.2	-1.3	-1.2	1.1	1

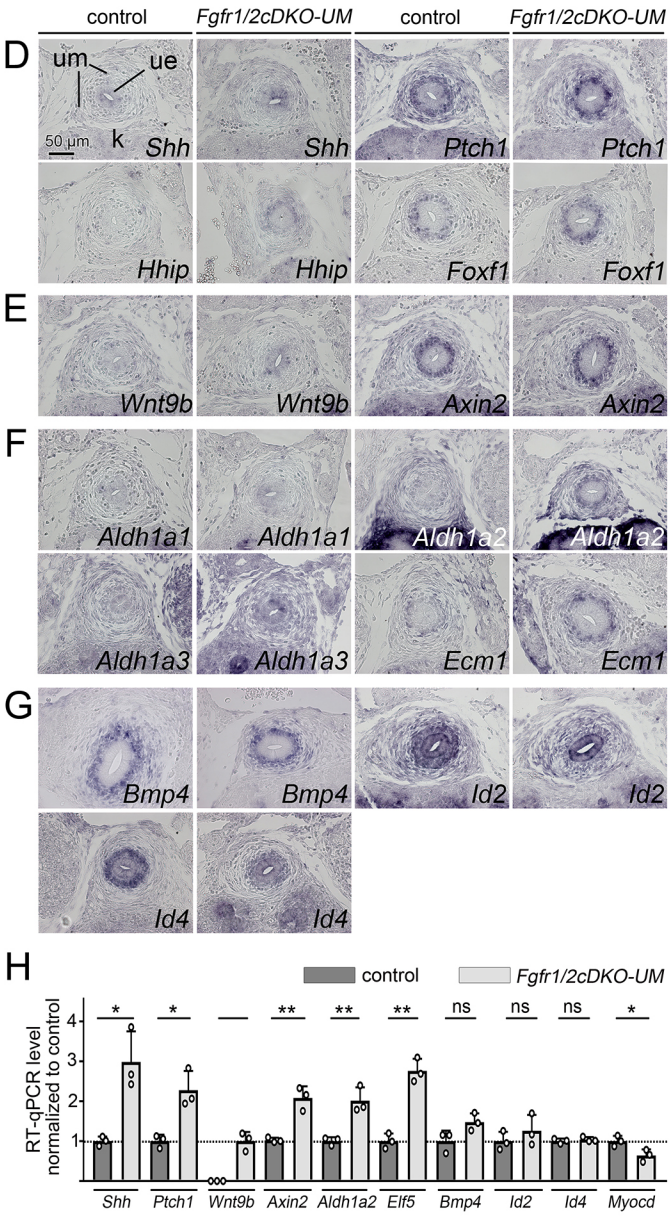

Fig. 4. Altered signaling activities in *Fgfr1/2cDKO-UM* ureters. (A) Pie chart summarizing the results from the microarray analysis of E14.5 control and *Fgfr1/2cDKO-UM* ureters. (B) Functional annotation clustering by DAVID for upregulated genes in the microarrays of E14.5 *Fgfr1/2cDKO-UM* ureters. (C) Changes of signaling components and activities in microarrays of E14.5 *Fgfr1/2cDKO-UM* and control ureters. Shown are the fold changes (FC) of four individual microarrays and the average FC. (D-G) RNA *in situ* hybridization analysis on transverse sections of E14.5 *Fgfr1/2cDKO-UM* and control ureters for expression of components and/or targets of SHH (D), WNT (E), RA (F) and BMP4 (G) signaling. $n \geq 3$ for each probe and genotype. k, kidney; ue, ureteric epithelium; um, ureteric mesenchyme. (H) RT-qPCR results for expression of genes encoding components and targets of SHH signaling (*Shh*, *Ptch1*), WNT signaling (*Wnt9b*, *Axin2*), RA signaling (*Aldh1a2*, *Elf5*), BMP4 signaling (*Bmp4*, *Id2*, *Id4*) and of *Myocd* in three independent RNA pools of E14.5 control and *Fgfr1/2cDKO-UM* ureters. Note that *Wnt9b* expression was normalized to the mutant because expression was not detectable in the control. *$P \leq 0.05$; **$P \leq 0.01$ (two-tailed Student's *t*-test). ns, not significant ($P > 0.05$). Values are shown as mean±s.d. For values and statistics, see Table S14A.

Development (2022) 149, dev200767. doi:10.1242/dev.200767

Axin2) (Bohnenpoll et al., 2017c; Trowe et al., 2012). Furthermore, genes encoding RA-synthesizing enzymes (*Aldh1a1*, *Aldh1a2*, *Aldh1a3*) were upregulated, as were direct targets of RA signaling activity in the UM (*Cyp26a1*, *Ecm1*) and in the UE (*Elf5*) (Bohnenpoll et al., 2017b). The effector gene of both SHH and WNT signaling, *Bmp4* (Bohnenpoll et al., 2017c; Mamo et al., 2017), was weakly upregulated (+1.2), whereas the direct target genes *Id2* and *Id4* (Hollnagel et al., 1999; Liu and Harland, 2003) were unchanged (Fig. 4C).

RNA *in situ* hybridization analysis confirmed increased expression of components and targets of SHH, WNT and RA signaling activity in E14.5 *Fgfr1/2cDKO-UM* ureters (Fig. 4D-F). Expression of *Bmp4* appeared unchanged whereas *Id2* and *Id4* expression was reduced in the UM (Fig. 4G).

Given that RNA *in situ* hybridization detected only weak expression changes, we performed reverse transcription-quantitative polymerase chain reaction (RT-qPCR) analysis for additional validation and quantification. We found an almost threefold increased expression of *Shh*, and a twofold increase of *Ptch1*. *Wnt9b*, *Axin2*, *Aldh1a2* and *Elf5* exhibited increased mRNA expression as well. *Bmp4* expression was unchanged, as was expression of *Id2* and *Id4*. The latter may reflect opposing changes of BMP4 signaling in the UE and UM. *Myocd* expression was significantly reduced (Fig. 4H, Table S14A). We conclude from these three independent assays that SHH, WNT and RA signaling are increased whereas BMP4 signaling is reduced in the mesenchymal compartment of *Fgfr1/2cDKO-UM* ureters at E14.5.

Mesenchymal FGFR1 and FGFR2 may act as a sink for FGF ligands

We recently reported that loss of epithelial *Fgfr2* expression leads to a decrease of *Shh* expression and of SHH, WNT and RA signaling activity in E14.5 ureters (Meuser et al., 2022), i.e. to molecular changes opposite to those found here for the mesenchymal knockout of *Fgfr1* and *Fgfr2*. In fact, the comparison of the list of genes with decreased expression in the epithelial *Fgfr2* knockout (*Pax2cre/+;Fgfr1*$^{fl/+}$*;Fgfr2*$^{fl/fl}$; *Fgfr1/2cDKO-UE*; note that *Fgfr1* was also deleted because of the chosen breeding strategy, but did not contribute to the described cellular and molecular changes) (Table S15) with that of genes with increased expression in the mesenchymal deletion of these receptor genes (*Tbx18*$^{cre/+}$*;Fgfr1*$^{fl/fl}$*;Fgfr2*$^{fl/fl}$; *Fgfr1/2cDKO-UM*) (Table S11) presented here, delivered an overlap of 47 genes (Fig. 5A). This overlap contained *Shh* and targets of its activity (*Hhip*, *Ptch1*, *Ptch2*), but also *Aldh1a3* and *Wnt9b*, suggesting that the increase of *Shh* expression, and of SHH, RA and WNT signaling is due to increased epithelial FGFR2 signaling in *Fgfr1/2cDKO-UM* ureters (Fig. 5B).

To substantiate this hypothesis, we analyzed expression of known direct targets of FGFR signaling, namely *Spry1* (Hanafusa et al., 2002) (microarray: +1.3) as well as *Etv4* and *Etv5* (Firnberg and Neubüser, 2002; Liu et al., 2003) (microarray: +1.2) in E14.5 *Fgfr1/2cDKO-UM* ureters by RNA *in situ* hybridization on sections. In fact, we found increased expression of *Spry1* in the UE. Mesenchymal expression of *Spry1* was not detected by this method (Fig. S9A). Section *in situ* hybridization was not sensitive enough to detect specific expression of *Etv4* and *Etv5* in the ureter at this stage, whereas in whole-mounts of E13.5 ureters cultured for 36 h an epithelial expression was apparent (Fig. S9B,C). Notably, expression of *Fgfr1* and *Fgfr2* appeared unchanged in the UE of E14.5 *Fgfr1/2cDKO-UM* embryos (Fig. S9D). RT-qPCR analysis confirmed increased expression of *Spry1*, *Etv4* and *Etv5*, with the latter reaching significance (Fig. 5C, Table S14B).

It is conceivable that in *Fgfr1/2cDKO-UM* ureters FGF ligands normally bound by the mesenchymal receptors excessively bind to epithelial FGFR2, thereby overactivating FGF signaling and, hence, *Shh* expression in the UE. We tested this hypothesis by treating explant cultures of E12.5 wild-type ureters for 18 h with 100 ng/µl of FGF10, the major ligand of FGFR2 (Igarashi et al., 1998; Jans, 1994). RT-qPCR detected an almost twofold increase in expression of *Shh*. Importantly, upon loss of *Fgfr1 and Fgfr2* in the epithelial compartment (in *Fgfr1/2cDKO-UE* ureters), *Shh* expression was reduced to 50% and could not be increased by FGF10, validating that FGF10 controls *Shh* expression via epithelial FGFR2 signaling (Fig. 5D, Table S14C).

Our *in situ* hybridization analysis revealed a decrease of mesenchymal expression of *Id2* and *Id4*, target genes of BMP4 signaling. We wondered whether altered expression of BMPR genes underlies this change. RNA section *in situ* hybridization analysis (with extended color development) provided the impression that *Bmpr1a*, *Bmpr1b* and *Bmpr2* exhibit increased expression in the epithelial compartment in *Fgfr1/2cDKO-UM* ureters at E14.5, but the level of expression of all of these genes was extremely low, making detection of changes by this method challenging (Fig. S9E). However, RT-qPCR analysis detected a 1.5-fold increase of expression of *Bmpr1a*, *Bmpr1b* and *Bmpr2* in E14.5 *Fgfr1/2cDKO-UM* ureters (Fig. 5E, Table S14D) and a 50% decrease in expression in *Fgfr1/2cDKO-UE* ureters at E14.5 (Fig. 5F, Table S14E). Moreover, E12.5 wild-type ureters cultured for 18 h with 100 ng/µl of FGF10 showed a slight but significant increase of *Bmpr1b* and *Bmpr2* expression (Fig. 5G, Table S14F). Together, this suggests that expression of BMPR genes in the UE is enhanced by epithelial FGFR2 signaling, which, in turn, is controlled by the amount of free FGF ligand, i.e. ligand not bound to mesenchymal FGFR1 and FGFR2.

A combination of increased SHH signaling and decreased BMP4 signaling recapitulates the phenotypic changes of *Fgfr1/2cDKO-UM* ureters

Our molecular analysis revealed increased SHH and decreased BMP4 signaling in the UM of *Fgfr1/2cDKO-UM*. To analyze the relative contribution of these changes to the delayed onset of SMC differentiation in mutant ureters, we treated explants of E13.5 wild-type ureters with 2 µM of the SHH signaling agonist purmorphamine (Li et al., 2008) and/or with the BMP4 antagonist noggin (NOG; 10 µg/ml) (Zimmerman et al., 1996) and scored peristaltic activity over an 8-day culture period. Addition of purmorphamine accelerated the onset of peristalsis by 1 day (starting at day 2-3 rather than at day 3-4 as in the control) whereas NOG-treated ureters acquired marginal peristaltic activity only after 7 days. Remarkably, a combination of the two treatments resulted in a delay of 1-2 days in the onset of peristaltic activity, similar to that observed in *Fgfr1/2cDKO-UM* ureters (Fig. 6A, Table S16A). Moreover, the contraction frequency of ureters treated with purmorphamine and NOG remained lower compared with that of control and of purmorphamine-treated ureters throughout the whole culture period (Fig. 6B, Table S16B).

Marker analysis revealed a premature onset at day 2 and an expansion of SMC differentiation upon purmorphamine treatment, whereas NOG abolished SMC markers in the ureter explants throughout the entire culture period. In the purmorphamine/NOG double-treated ureters, SMC differentiation was reduced at day 4 but was prominent and expanded at the endpoint at day 8.

Development (2022) 149, dev200767. doi:10.1242/dev.200767

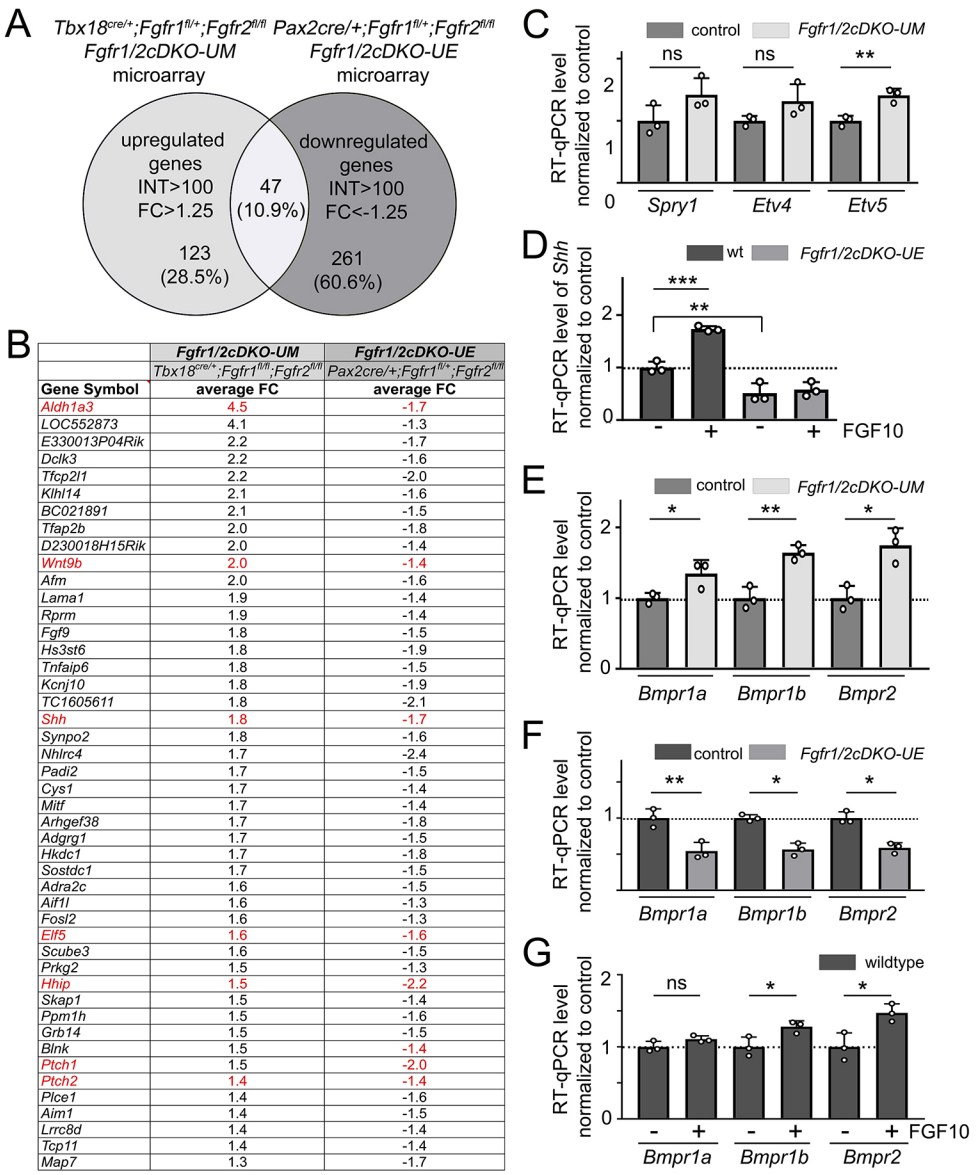

B

	Fgfr1/2cDKO-UM	Fgfr1/2cDKO-UE
	Tbx18cre/+;Fgfr1fl/fl;Fgfr2fl/fl	Pax2cre/+;Fgfr1fl/+;Fgfr2fl/fl
Gene Symbol	**average FC**	**average FC**
Aldh1a3	4.5	-1.7
LOC552873	4.1	-1.3
E330013P04Rik	2.2	-1.7
Dclk3	2.2	-1.6
Tfcp2l1	2.2	-2.0
Klhl14	2.1	-1.6
BC021891	2.1	-1.5
Tfap2b	2.0	-1.8
D230018H15Rik	2.0	-1.4
Wnt9b	2.0	-1.4
Afm	2.0	-1.6
Lama1	1.9	-1.4
Rprm	1.9	-1.4
Fgf9	1.8	-1.5
Hs3st6	1.8	-1.9
Tnfaip6	1.8	-1.5
Kcnj10	1.8	-1.9
TC1605611	1.8	-2.1
Shh	1.8	-1.7
Synpo2	1.8	-1.6
Nhlrc4	1.7	-2.4
Padi2	1.7	-1.5
Cys1	1.7	-1.4
Mitf	1.7	-1.4
Arhgef38	1.7	-1.8
Adgrg1	1.7	-1.5
Hkdc1	1.7	-1.8
Sostdc1	1.7	-1.5
Adra2c	1.6	-1.5
Aif1l	1.6	-1.3
Fosl2	1.6	-1.3
Elf5	1.6	-1.6
Scube3	1.6	-1.5
Prkg2	1.5	-1.3
Hhip	1.5	-2.2
Skap1	1.5	-1.4
Ppm1h	1.5	-1.6
Grb14	1.5	-1.5
Blnk	1.5	-1.4
Ptch1	1.5	-2.0
Ptch2	1.4	-1.4
Plce1	1.4	-1.6
Aim1	1.4	-1.5
Lrrc8d	1.4	-1.4
Tcp11	1.4	-1.4
Map7	1.3	-1.7

Fig. 5. Loss of mesenchymal *Fgfr1* and *Fgfr2* expression leads to increased epithelial FGFR2 signaling. (A) Diagram showing the large overlap of genes upregulated in the microarray of the mesenchymal *Fgfr1/2* knockout (*Fgfr1/2cDKO-UM*; *Tbx18*$^{cre/+}$;*Fgfr1*$^{fl/fl}$;*Fgfr2*$^{fl/fl}$) and downregulated in the epithelial knockout of *Fgfr1/2* in the ureter at E14.5 (*Fgfr1/2cDKO-UE*; *Pax2cre/+;Fgfr1*$^{fl/+}$;*Fgfr2*$^{fl/fl}$). For complete gene lists, see Tables S11 and S15. (B) List of 47 genes from the overlap of the gene lists shown in A. Genes marked in red are components and/or targets of SHH signaling (*Shh*, *Hhip*, *Ptch1*, *Ptch2*), RA signaling (*Aldh1a3*, *Elf5*) and WNT signaling (*Wnt9b*). (C) RT-qPCR results for expression of *Spry1*, *Etv4* and *Etv5* in three independent RNA pools of E14.5 control and *Fgfr1/2cDKO-UM* ureters. **$P \leq 0.01$ (two-tailed Student's *t*-test). For values and statistics, see Table S14B. (D) RT-qPCR results for expression of *Shh* in three independent RNA pools each of explants of E12.5 wild-type and *Fgfr1/2cDKO-UE* ureters treated with 100 ng/µl FGF10 for 18 h; **$P \leq 0.01$; ***$P \leq 0.001$ (two-way ANOVA followed by Tukey's multiple comparisons test; selected comparisons with significant difference shown). For values and complete statistics, see Table S14C. (E) RT-qPCR results for expression of BMPR genes in three independent RNA pools of E14.5 control and *Fgfr1/2cDKO-UM* ureters. *$P \leq 0.05$; **$P \leq 0.01$ (two-tailed Student's *t*-test). For values and statistics, see Table S14D. (F) RT-qPCR results for expression of BMPR genes in three independent RNA pools of E14.5 control and *Fgfr1/2cDKO-UE* ureters. *$P \leq 0.05$; **$P \leq 0.01$ (two-tailed Student's *t*-test). For values and statistics, see Table S14E. (G) RT-qPCR results for expression of BMPR genes in three independent RNA pools each of explants of E12.5 wild-type ureters treated with 100 ng/µl FGF10 for 18 h. *$P \leq 0.05$ (two-tailed Student's *t*-test). For values and statistics, see Table S14F. Values in C-G are shown as mean ±s.d. FC, fold change; INT, intensity; ns, not significant; wt, wild type.

Purmorphamine treatment enhanced ALDH1A2 expression as did the loss of BMP4 signaling at day 2, whereas purmorphamine/NOG treatment led to an expanded peri-epithelial ALDH1A2 domain at the endpoint, again recapitulating the observation in *Fgfr1/2cDKO-UM* ureters (Fig. 6C). Together, we conclude that a combination of increased SHH signaling and decreased BMP4 signaling recapitulates the phenotypic changes of *Fgfr1/2cDKO-UM* ureters (Fig. 7).

DISCUSSION

FGFR1 and FGFR2 maintain the structural and functional integrity of the ureter by patterning the UM

We addressed FGFR1 and FGFR2 function in the UM by a specific conditional gene-targeting approach based on the exclusive expression of *Tbx18* in this tissue (Bohnenpoll et al., 2013). Combined mesenchymal loss of *Fgfr1* and *Fgfr2* by our *Tbx18*^{cre} knock-in line (Airik et al., 2010) resulted in hydroureter formation

Development (2022) 149, dev200767. doi:10.1242/dev.200767

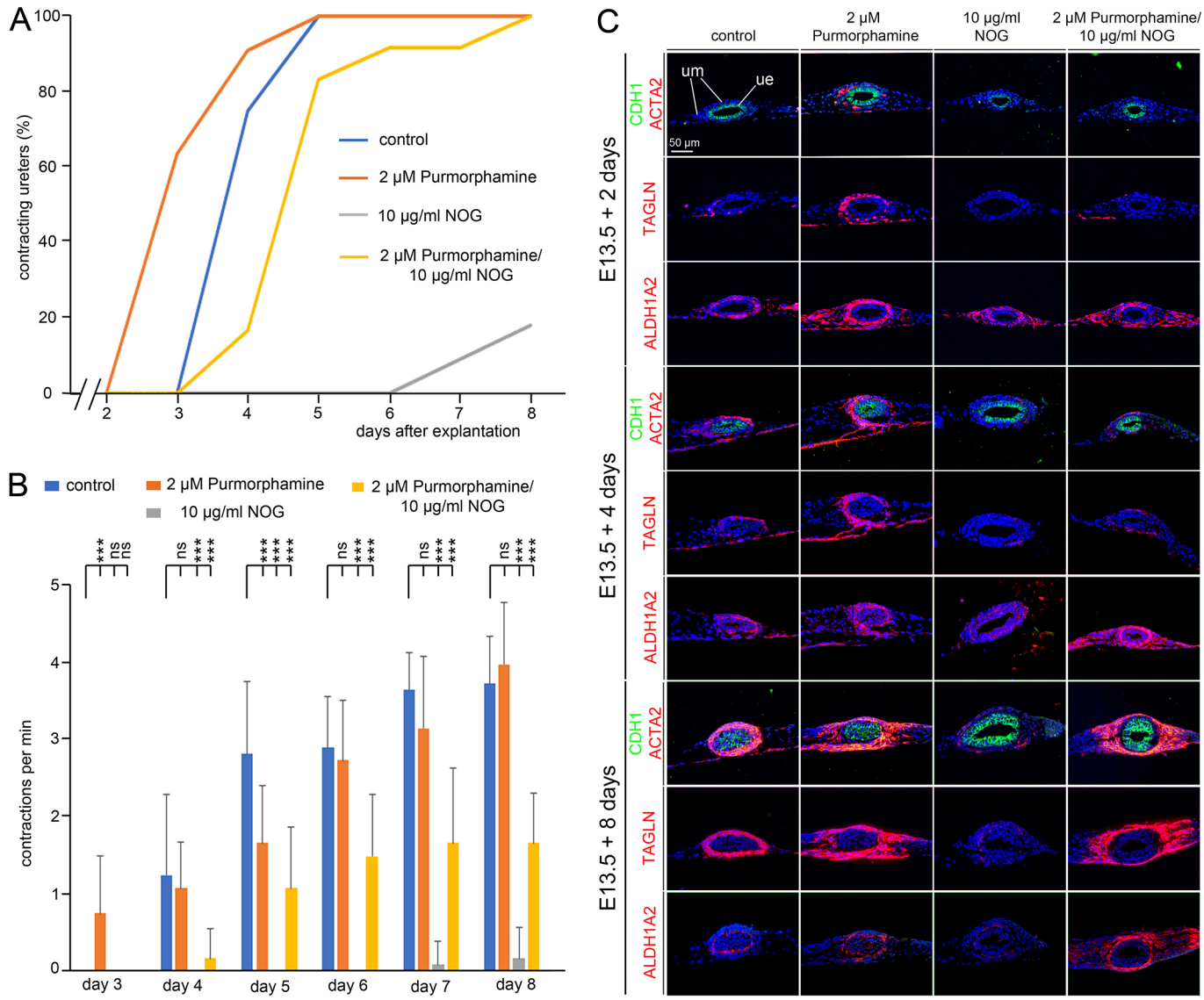

Fig. 6. The combination of increased SHH and reduced BMP4 signaling recapitulates the phenotypic changes of *Fgfr1/2cDKO-UM* ureters. (A-C) Wild-type ureters were explanted at E13.5 and cultured for 8 days in minimal medium supplemented with DMSO (control, *n*=12), 2 µM purmorphamine (*n*=11), 10 µg/ml NOG (*n*=11) or 2 µM purmorphamine with 10 µg/ml NOG (*n*=12) and analyzed for peristaltic activity and SMC differentiation. (A) Graph showing the percentage of contracting ureters at different time points of the culture. (B) Graph of the contraction frequency (per min) at day 3-8 of the culture. Values are shown as mean±s.d. ***P<0.001 (two-tailed Student's t-test). For detailed values, see Table S16. (C) (Co-)immunofluorescence analysis of expression of the epithelial marker CDH1 together with the SMC marker ACTA2, of the SMC marker TAGLN, and of the lamina propria marker ALDH1A2 on transverse section of E13.5 ureter explants cultured for 2, 4 and 8 days. Nuclei are counterstained (in blue) with DAPI. *n*=5 for each marker, genotype and stage. ue, ureteric epithelium; um, ureteric mesenchyme.

but did not affect the overall composition of the excretory system and the integrity and size of its other major organs, the kidney and the bladder. The luminal path from the pelvis to the bladder was unaffected. Moreover, we did not find gross urothelial defects in *Fgfr1/2cDKO-UM* ureters. Absence of these phenotypic traits not only proves that hydroureter in *Fgfr1/2cDKO-UM* embryos arises from functional insufficiency of the outer mesenchymal coat, it also confirms that mesenchymal and epithelial lineages outside the UM were not affected to any substantial degree by our conditional targeting approach.

Our breeding strategy only allowed for recovery of *Fgfr1* and *Fgfr2* compound mutants for phenotypic analysis. However, the genotype-phenotype correlation clearly argues that loss of *Fgfr2* is the dominant factor for hydroureter formation, but that loss of *Fgfr1* contributed at least partly to this morphological defect.

Owing to postnatal lethality of *Fgfr1/2cDKO-UM* mice we could not analyze adolescent or adult mice for uro- and nephropathy. However, we assume that the hydroureter worsens leading to dilatation of the pelvis and the renal collecting system (hydronephrosis), a condition that would ultimately destroy the renal parenchyma. *Fgfr1/2cDKO-UM* ureters regained considerable peristaltic performance when relieved from urinary pressure in an *ex vivo* culture setting. Although this confirms that increased hydrostatic pressure exacerbates the SMC defects *in vivo*, it suggests that *in vivo* a temporary artificial bypass may provide a means for (re-)differentiation of contractile SMCs and a regain of peristaltic activity. Irrespective of such a therapeutic option for a subgroup of congenital forms of hydroureter in human patients, *Fgfr1 and Fgfr2* present relevant candidates to include in mutational screens for genetic causes of this disease entity.

Development (2022) 149, dev200767. doi:10.1242/dev.200767

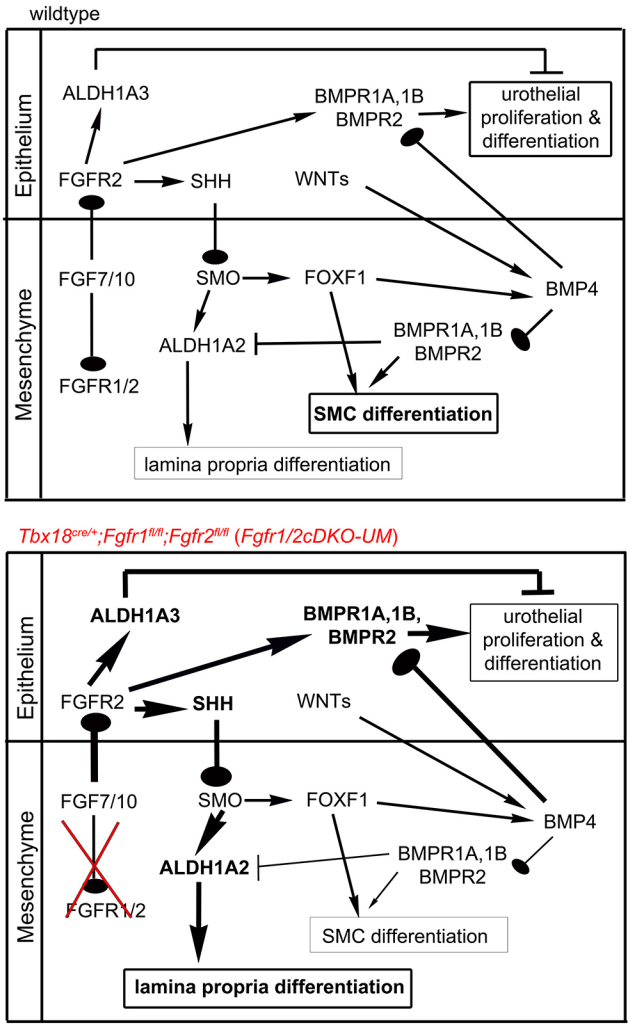

Fig. 7. Model of how mesenchymal FGFR1 and FGFR2 expression regulates various signaling pathways to assure normal patterning and SMC differentiation of the UM around E14.5. Top: In the wild type, mesenchymal FGFR1 and FGFR2 compete with epithelial FGFR2 for binding to FGF7 and FGF10. This dampens the expression of *Aldh1a3*, *Shh* and BMPR genes by epithelial FGFR2 signaling. BMP4 in the mesenchyme represses *Aldh1a2* expression and, together with FOXF1, activates SMC differentiation leading in sum to SMC differentiation around E14.5, whereas lamina propria fibrocyte differentiation is suppressed. Bottom: Loss of mesenchymal FGFR1 and FGFR2 (*Tbx18*$^{cre/+}$;*Fgfr1*$^{fl/fl}$;*Fgfr2*$^{fl/fl}$; *Fgfr1/2cDKO-UM*, marked in red) leads to overactivation of epithelial FGFR2 signaling and enhanced epithelial expression of *Shh*, BMPR genes and *Aldh1a3*. Increased SHH signaling leads to increased expression of *Aldh1a2* in the mesenchyme. BMP4 binding shifts to epithelial BMPR. Less BMP4 is available in the mesenchyme to repress *Aldh1a2* and to activate the SMC program leading to premature lamina propria formation at E14.5. The effects on epithelial development are minor because the inhibitory effect of RA on differentiation is counteracted by increased epithelial BMPR signaling. Arrows indicate activating interactions, ovals ligand receptor interaction, bars inhibitory interactions. The width of arrows, bars and boxes indicates the relative level of activation.

Our cellular and molecular profiling detected decreased proliferation, delayed SMC differentiation and precocious lamina propria formation in *Fgfr1/2cDKO-UM* ureters. Analyses of other mouse models revealed that a 1-day delay in activation of *Myocd* and SMC structural genes does not compromise ureter integrity whereas a delay of two or more days leads to hydroureter formation (Kurz et al., 2022; Weiss et al., 2019). This relates to the onset of urine production in the kidney around E16.5, which generates a hydrostatic pressure that widens the ureter when SMCs are absent at this time point. Given our finding that SMC differentiation is delayed by 1 day in *Fgfr1/2cDKO-UM* ureters, we assume that precocious lamina propria formation contributed to hydroureter formation. This may occur by deposition of extracellular matrix that compromises SMC coupling or by the emergence of a 'myofibroblastic' cell type that lacks the contractile strength of SMCs.

Although the ureter and bladder arise from different primordia in different germ layers, the role of *Fgfr1* and *Fgfr2* seems to be conserved in the early development of these organs. Loss of *Fgf7* led to urothelial stratification defects in the bladder (Tash et al., 2001), and conditional deletion of *Fgfr2* in the bladder mesenchyme resulted in expansion of the lamina propria at the expense of the SMC layer (Ikeda et al., 2017). We posit that integration of FGF signaling in the epithelial and mesenchymal primordia of these organs contributed during evolution to the structural and functional divergence from components of the renal drainage system, the collecting ducts and the pelvis, that preserved a mono-layered epithelial lining and (myo)fibroblastic character of the surrounding mesenchyme.

The combination of increased SHH and decreased BMP4 signaling accounts for defects in mesenchymal patterning in *Fgfr1/2cDKO-UM* ureters

Our molecular profiling experiments identified altered activities of a number of signaling pathways that had previously been implicated in the development of the UM (Bohnenpoll et al., 2017b,c; Mamo et al., 2017; Trowe et al., 2012). SHH, WNT and RA signaling were increased whereas BMP4 signaling was decreased in the UM at E14.5, i.e. prior to onset of differentiation of SMCs and lamina propria fibrocytes. Increased SHH signaling was also detected in E16.5 bladders lacking mesenchymal *Fgfr2* expression but the activity of the other pathways was not analyzed in that context (Ikeda et al., 2017).

The work of several labs has identified SHH signaling as a crucial pathway for mesenchymal proliferation and SMC differentiation in both the bladder and the ureter (Bohnenpoll et al., 2017c; Cao et al., 2010; Shiroyanagi et al., 2007; Yu et al., 2002). Yu et al. reported that ureters with conditional deletion of *Shh* from the UE not only lacked the SMC layer but were also deficient for the lamina propria. Based on the finding that SHH administration to isolated UM led to SMC induction at low doses only, they concluded that the patterning of the UM into an inner layer of lamina propria fibrocytes and outer SMCs depends on a SHH signaling gradient (Yu et al., 2002). A similar finding was reported for the bladder mesenchyme (Cao et al., 2010).

Although this interpretation seems plausible at first sight, it is clearly not supported by the profile of *Shh* expression in the ureter. *Shh* expression in the UE is relatively high from E11.5 to E14.5 when *Myocd* induction occurs and SMC differentiation starts, but drops sharply thereafter and only rises to low levels from E18.5 onwards when lamina propria fibrocytes emerge in the innermost region of the UM (Bohnenpoll et al., 2017c). Our ureter explant culture experiments showed that increased SHH signaling (triggered by administration of purmorphamine to E12.5 ureters) leads to premature expression of SMC markers after 2 days and a widening of the SMC layer after 8 days, incompatible with the previous notion that high doses of SHH inhibit SMC differentiation. Remarkably, increased SHH signaling resulted in a strongly increased and overlapping expression of ALDH1A2, an RA biosynthetic enzyme

Development (2022) 149, dev200767. doi:10.1242/dev.200767

and lamina marker, after 2 days, suggesting that SHH signaling induces SMC and lamina fates simultaneously. ALDH1A2 expression largely extended into the outer region of the UM, in which expression of SMC markers was absent, suggesting that additional signals are required to induce SMCs close to the UE or to prevent this differentiation in the outer region.

Inhibition of BMP4 signaling with NOG resulted in a complete loss of SMC differentiation, and increased ALDH1A2 expression after 2 days, but not thereafter. This supports our previous findings that BMP4 signaling is essential for SMC differentiation and cooperates with SHH signaling (Bohnenpoll et al., 2017c). It also points out that BMP4 signaling represses ALDH1A2 expression induced by endogenous SHH signaling. Finally, combinatorial activation of SHH and inhibition of BMP4 resulted in ectopic and increased ALDH1A2 expression starting after 2 days and a delayed onset of SMC differentiation.

We previously showed that RA is sufficient to increase expression of *Wnt9b* in the UE and enhance WNT signaling activity in the UM in explant cultures of ureters (Bohnenpoll et al., 2017b). Together with our current finding that forced ectopic activation of SHH signaling induces expression of ALDH1A2, we deduce that increased RA and WNT signaling in *Fgfr1/2cDKO-UM* ureters results from the increase of *Shh* expression in the UE. However, increased RA signaling may contribute to delayed SMC differentiation and account for reduced expression of components and regulators of S-cell differentiation at E14.5, as previously reported (Bohnenpoll et al., 2017b).

We conclude that the major phenotypic traits of *Fgfr1/2cDKO-UM* ureters – delayed SMC differentiation and premature and expanded lamina propria formation – are due to a combination of increased SHH and decreased BMP signaling in the UM. Our findings confirm our previous results that SMC differentiation is promoted by combined SHH and BMP4 signaling activities and, surprisingly, suggest that lamina development is induced by SHH signaling but requires absence of BMP4 signaling.

The molecular function of FGFR1 and FGFR2 in the UM: limitation of FGF ligands for activation of epithelial FGFR2 signaling

Molecular analysis of fetal bladders with loss of *Fgfr2* in the mesenchymal compartment revealed that increased mesenchymal SHH signaling was not associated with increased epithelial *Shh* expression but correlated with increased mesenchymal expression of the genes *Boc* and *Cdon*, which encode PTCH1 co-receptors. It was concluded that FGFR2 signaling normally dampens *Cdon* and *Boc* expression and SHH signaling activity in bladder mesenchyme for proper patterning of the muscle and lamina propria (Ikeda et al., 2017).

Although our transcriptional profiling experiment found increased SHH signaling activity in the UM, we did not find alterations in *Boc* and *Cdon* expression in our microarray. However, and in clear contrast to the situation in the developing bladder, our microarrays detected increased expression of *Shh*, which we confirmed in two independent assays. This suggests that increased SHH signaling in the UM results from increased *Shh* expression in the UE.

This '*trans*' effect of mesenchymal *Fgfr1* and *Fgfr2* loss might be due to a complicated feedback mechanism employing a mesenchymally expressed secondary signal. However, our findings rather point towards a role of mesenchymal FGFR1 and FGFR2 to limit the concentration of FGF ligands for activation of FGFR2-mediated *Shh* transcription in the UE. First, loss of mesenchymal *Fgfr1* and *Fgfr2* led to increased FGF signaling activity in the adjacent UE (read-out: *Spry1*, *Etv4*, *Etv5*). Second, loss of epithelial *Fgfr2* resulted in decreased *Shh* expression, and decreased SHH, RA and WNT signaling activity in the UM (Meuser et al., 2022), i.e. to molecular changes opposite to those observed in the mesenchymal *Fgfr1* and *Fgfr2* deletion. Third, administration of FGF10, the primary ligand of FGFR2, to ureter explants led to increased *Shh* expression but only when FGFR2 was present in the epithelium. Fourth, and finally, our recent study showed that expression of *Spry1*, a transcriptional target of FGF signaling activity, in the UE is dependent on epithelial FGFR2 signaling but cannot be detected by *in situ* hybridization analysis in the UM (Meuser et al., 2022), indicating that mesenchymal FGFR1 and FGFR2 signaling elicits no or only a minor transcriptional response in this tissue.

Our *in situ* hybridization results revealed reduced expression of the BMP target genes *Id2* and *Id4* in the UM of *Fgfr1/2cDKO-UM* embryos. Although the sensitivity of this method was not sufficient to detect changes of *Id2/Id4* expression in the UE, it is conceivable that epithelial BMP4 signaling, and hence target gene expression, is enhanced considering the overall unchanged *Id2/Id4* levels both in our microarrays and in RT-qPCR analysis of whole *Fgfr1/2cDKO-UM* ureters.

There are (at least) two possible explanations for the regulation of BMP signaling in the ureter by mesenchymal FGFR1 and FGFR2. First, it is conceivable that mesenchymal FGFR1 and FGFR2 exert a (weak) signaling activity to enhance BMP signaling in the UM. This may be achieved in a transcription-independent manner, e.g. by downstream kinases that activate components and effectors of the BMP signaling machinery, or in a transcription-dependent manner, e.g. by enhancing expression of genes encoding BMP signaling components in the UM. In this scenario, loss of FGFR1 and FGFR2 signaling function in the UM would lead to reduced mesenchymal BMP4 signaling and more BMP4 would be available to bind to and activate BMP4 receptors in the UE.

Alternatively, mesenchymal FGFR1 and FGFR2 may again, as explained before for *Shh* expression, act as a sink for FGFs to control activation of FGFR2 signaling in the UE. Here, epithelial FGFR2 should control expression of genes encoding components of epithelial BMP signaling, such as BMP4 receptor genes in the UE. Loss of mesenchymal FGFR1 and FGFR2 would lead to increased expression of epithelial BMP4 receptors, which could outcompete mesenchymal BMP4 receptors for binding the limited amount of BMP4 ligand.

Although we cannot rule out that mesenchymal FGFR1 and FGFR2 exert a weak signaling activity that controls mesenchymal BMP4 signaling, our findings favor a 'sink' role for mesenchymal FGFR1 and FGFR2. Expression of all three BMPR genes (*Bmpr1a*, *Bmpr1b*, *Bmpr2*) was decreased in *Fgfr1/2cDKO-UE* ureters and increased in *Fgfr1/2cDKO-UM* ureters at E14.5, and exogenous FGF10 caused increased expression of the receptor genes, compatible with the notion that epithelial FGFR2 signaling activity enhances expression of these receptor genes, whereas mesenchymal FGFR1 and FGFR2 limit epithelial activation of these genes by limiting FGF ligand availability.

Together, our findings suggest that FGFR1 and FGFR2 exert a largely signaling-independent function in the UM by binding of FGF ligands and preventing them from activating FGFR2 in the UE. This balances SHH and BMP4 signaling and favors the differentiation of the inner region of the UM into SMCs, which is crucial to maintain the integrity of the ureter (Fig. 7).

Development (2022) 149, dev200767. doi:10.1242/dev.200767

MATERIALS AND METHODS

Mice

Mice with *loxP* sites flanking exon 4 of the *Fgfr1* locus (*Fgfr1*$^{tm5.1Sor}$; synonym: *Fgfr1*^{fl}) (Hoch and Soriano, 2006), and mice with *loxP* sites flanking exons 8-10 of the *Fgfr2* locus (*Fgfr2*^{tm1Dor}; synonym: *Fgfr2*^{fl}) (Yu et al., 2003) were obtained from The Jackson Laboratory. *Tbx18*$^{tm4(cre)Akis}$ (synonym: *Tbx18*^{cre}) mice used for recombination in the mesenchymal progenitors of the ureter (Bohnenpoll et al., 2013) were previously generated in the lab (Airik et al., 2010), as were *Tg(Pax2-cre)1AKis* (synonym: *Pax2-cre*) mice for recombination in the UE (Bohnenpoll et al., 2017a; Trowe et al., 2011). All mice were maintained on an NMRI outbred background. Mutant embryos were generated by mating *Tbx18*$^{cre/+}$;*Fgfr1*$^{fl/+}$;*Fgfr2*$^{fl/+}$ or *Pax2-cre*/+$^{/+}$;*Fgfr1*$^{fl/+}$;*Fgfr2*$^{fl/+}$ males with *Fgfr1*$^{fl/fl}$;*Fgfr2*$^{fl/fl}$ females. *Cre*-negative littermates were used as controls. For timed pregnancies, vaginal plugs detected in the morning after mating were designated as E0.5 at noon. Urogenital systems and embryos were dissected in PBS, fixed in 4% paraformaldehyde in PBS and stored in methanol at −20°C. Genotyping was performed by PCR on genomic DNA prepared from yolk sacs, embryo tissues or ear clips.

Mice were housed in rooms with controlled light and temperature at the central animal laboratory of the Medizinische Hochschule Hannover. The experiments were in accordance with the German Animal Welfare Legislation and approved by the local Institutional Animal Care and Research Advisory Committee and permitted by the Lower Saxony State Office for Consumer Protection and Food Safety (AZ 33.12-42502-04-13/1356, AZ42500/1H).

Organ cultures and peristalsis assays

Ureters from murine embryos of different stages were dissected in L-15 Leibovitz medium (F1315, Biochrom), explanted on 0.4 µm polyester membrane Transwell supports (3450, Corning) and cultured at the air-liquid interface. Explants were cultured in DMEM/F12 (21331020, Gibco) with 1× penicillin/streptomycin (15140122, Gibco), 1× pyruvate (11360070, Gibco) and 1× GlutaMAX (35050038, Gibco) in a humidified incubator with 5% CO_2 at 37°C. For cultures of *Fgfr1/2cDKO-UM* ureters, we added 10% fetal calf serum (Biochrom) to the medium.

For pharmacological perturbation experiments, we dissolved the following compounds in DMSO or ddH_2O and used them at the indicated final concentrations: eukaryotic FGF10 (100 ng/µl, in ddH_2O; USC-EPB882HU61-10, BIOZOL), purmorphamine (2 µM, in DMSO; 540220, Merck), noggin (10 µg/ml, in ddH_2O; ZO3205, BIOZOL/GenScript). Medium was refreshed every second day.

For evaluating contraction frequency and intensity of cultured ureters, 1 min videos of each ureter were taken using a frame rate of 5 per sec with a Leica DM6000 microscope with Leica DFC350FX digital camera and analyzed using Fiji (Schindelin et al., 2012). The contraction intensity was analyzed at 25%, 50% and 75% of the total ureter length by calculating the relative width of the ureter during contraction and relaxation. Graphs were plotted in Microsoft Excel v.14 (Microsoft Corporation).

Histological and immunohistochemical analyses

Embryos, urogenital systems and ureter explants were fixed in 4% paraformaldehyde, paraffin wax embedded and sectioned at 5 µm. Sections were stained with Hematoxylin and Eosin according to standard procedures.

Immunofluorescence staining was performed on 5-µm paraffin wax sections using the following primary antibodies and dilutions: polyclonal rabbit anti-KRT5 (1:250; PRB-160P, BioLegend), polyclonal rabbit anti-ΔNP63 (1:250; clone Poly6190, 619001, BioLegend), monoclonal mouse anti-UPK1B (1:250; clone1E1, WH0007348M2, Sigma-Aldrich), polyclonal rabbit anti-TAGLN (1:200; ab14106, Abcam), polyclonal rabbit anti-ACTA2 (1:200, A5228; clone 1A4; Merck), polyclonal rabbit anti-ALDH1A2 (1:200; ab75674, Abcam), polyclonal rabbit anti-CDH1 (a kind gift from Dr R. Kemler, MPI, Freiburg, Germany) and monoclonal mouse anti-BrdU (1:250; 1170376, clone BMC9318, Roche). Fluorescent staining was performed using the following secondary antibodies: biotinylated goat anti-rabbit IgG (1:200; 111065033, Dianova), biotinylated donkey anti-goat IgG (1:200; 705-065-003; Dianova), biotinylated goat anti-mouse IgG (1:200; 115-065-166, Jackson ImmunoResearch), Alexa 488-conjugated goat anti-rabbit IgG (1:500; A11034, Molecular Probes) and Alexa 555-conjugated goat anti-mouse IgG (1:500; A21422, Molecular Probes). The signals of ΔNP63 and ALDH1A2 were amplified using the Tyramide Signal Amplification system (NEL702001KT, Perkin Elmer). For antigen retrieval, paraffin sections were deparaffinized, pressure-cooked for 20 min in antigen unmasking solution (H3300, Vector Laboratories), treated with 3% H_2O_2/PBS for blocking of endogenous peroxidases, washed in PBST (0.05% Tween-20 in PBS) and incubated in TNB Blocking Buffer (NEL702001KT, Perkin Elmer). Sections were then incubated with primary antibodies at 4°C overnight. Nuclei were stained with 4′,6-diamidino-2-phenylindole (DAPI; 6335.1, Carl Roth). At least three specimens of each genotype were used for each analysis.

Cellular assays

In vivo cell proliferation rates were assayed by detection of incorporated BrdU on 5-µm paraffin wax sections (Bussen et al., 2004). Twelve sections of each specimen (n=3) were analyzed. The BrdU labeling index was defined as the number of BrdU-positive nuclei relative to the total number of nuclei detected by DAPI counterstaining in histologically defined compartments of the ureter.

Apoptosis in tissues was evaluated by the TUNEL assay using ApopTag Plus Fluorescein In Situ Apoptosis Detection Kit (S7111; Merck) on 5-µm paraffin sections.

RNA *in situ* hybridization analysis

Non-radioactive *in situ* hybridization analysis of gene expression was performed on 10-µm transversal paraffin wax sections of the proximal ureter using digoxigenin-labeled antisense riboprobes as previously described (Moorman et al., 2001).

RT-qPCR

RNA extraction and RT-qPCR analysis for gene expression was performed on three independent pools of 20 ureters each of E14.5 control, *Fgfr1/2cDKO-UM* and *Fgfr1/2cDKO-UE* embryos or of ten ureters each of E12.5 control and *Fgfr1/2cDKO-UE* embryos after 18 h of culture as previously described (Meuser et al., 2022). Primers are listed in Table S17.

Microarray analysis

For microarray analysis, ureters were either isolated at E15.5, explanted on Transwell membranes, cultivated for 6 days and then stored at −80°C or were isolated at E14.5 and directly frozen and stored at −80°C. Two independent pools of control and mutant ureters (five ureters each from male and female embryos) were collected for the E15.5+6 day microarray. Four independent pools of control and mutant ureters (20 ureters each for male and female embryos) were used for microarray analysis at E14.5. Total RNA from each pool was extracted using peqGOLD RNApure (30-1010, VWR International) and subsequently processed by the Research Core Unit Transcriptomics of Hannover Medical School. Whole Mouse Genome Oligo v2 (4×44K) Microarrays (G4846A; Agilent Technologies) were used for transcriptome analysis. Normalized expression data were filtered using Microsoft Excel (Microsoft Corporation). Functional enrichment analysis for up- and downregulated genes was performed with DAVID 6.8 web-software (https://david.ncifcrf.gov/) using default settings, and terms were selected based on *P*-value.

Statistics

Statistical analysis was performed using unpaired, two-tailed Student's *t*-test or a two-way analysis of variance (ANOVA) followed by Tukey's multiple comparisons test as indicated (GraphPad Prism version 7.03 and Microsoft Excel). Values are presented as mean±s.d. with P<0.05 considered significant.

Image documentation

Sections were photographed using a DM5000 microscope (Leica Camera, Wetzlar, Germany) with Leica DFC300FX digital camera or a Leica

DMI6000B microscope with Leica DFC350FX digital camera. All images were then processed in Adobe Photoshop CS3 or CS4.

Acknowledgements
We thank Rolf Kemler (MPI for Immunobiology, Freiburg) for the CDH1 antibody, and Patricia Zarnovican for excellent technical support. Microarray data used in this publication were generated by the Research Core Unit Genomics (RCUG) at Hannover Medical School.

Competing interests
The authors declare no competing or financial interests.

Author contributions
Conceptualization: L.D., H.T., A.K.; Methodology: M.M., H.T., M.-O.T.; Software: M.-O.T.; Validation: L.D., H.T.; Formal analysis: L.D., M.M., H.T., U.W.H.J., M.-O.T.; Investigation: L.D., M.M., H.T., U.W.H.J., C.R., M.-O.T.; Resources: C.R.; Data curation: L.D., H.T., M.-O.T.; Writing - original draft: L.D., A.K.; Writing - review & editing: L.D., M.M., H.T., U.W.H.J., C.R., H.H., M.-O.T., A.K.; Visualization: L.D., H.T.; Supervision: C.R., H.H., A.K.; Project administration: A.K.; Funding acquisition: H.H., A.K.

Funding
This work was supported by a grant from the German Research Council (Deutsche Forschungsgemeinschaft; DFG KI728/9-2) to A.K.

Data availability
Microarray data have been deposited in Gene Expression Omnibus under accession numbers GSE197368 and GSE197369.

Peer review history
The peer review history is available online at https://journals.biologists.com/dev/lookup/doi/10.1242/dev.200767.reviewer-comments.pdf.

References
Airik, R., Trowe, M.-O., Foik, A., Farin, H. F., Petry, M., Schuster-Gossler, K., Schweizer, M., Scherer, G., Kist, R. and Kispert, A. (2010). Hydroureternephrosis due to loss of Sox9-regulated smooth muscle cell differentiation of the ureteric mesenchyme. *Hum. Mol. Genet.* **19**, 4918-4929. doi:10.1093/hmg/ddq426

Aydoğdu, N., Rudat, C., Trowe, M.-O., Kaiser, M., Lüdtke, T. H., Taketo, M. M., Christoffels, V. M., Moon, A. and Kispert, A. (2018). TBX2 and TBX3 act downstream of canonical WNT signaling in patterning and differentiation of the mouse ureteric mesenchyme. *Development* **145**, dev171827. doi:10.1242/dev.171827

Baskin, L. S., Hayward, S. W., Young, P. and Cunha, G. R. (1996). Role of mesenchymal-epithelial interactions in normal bladder development. *J. Urol.* **156**, 1820-1827. doi:10.1016/S0022-5347(01)65545-9

Bohnenpoll, T. and Kispert, A. (2014). Ureter growth and differentiation. *Semin. Cell Dev. Biol.* **36**, 21-30. doi:10.1016/j.semcdb.2014.07.014

Bohnenpoll, T., Bettenhausen, E., Weiss, A.-C., Foik, A. B., Trowe, M.-O., Blank, P., Airik, R. and Kispert, A. (2013). Tbx18 expression demarcates multipotent precursor populations in the developing urogenital system but is exclusively required within the ureteric mesenchymal lineage to suppress a renal stromal fate. *Dev. Biol.* **380**, 25-36. doi:10.1016/j.ydbio.2013.04.036

Bohnenpoll, T., Feraric, S., Nattkemper, M., Weiss, A.-C., Rudat, C., Meuser, M., Trowe, M.-O. and Kispert, A. (2017a). Diversification of cell lineages in ureter development. *J. Am. Soc. Nephrol.* **28**, 1792-1801. doi:10.1681/ASN.2016080849

Bohnenpoll, T., Weiss, A.-C., Labuhn, M., Lüdtke, T. H., Trowe, M.-O. and Kispert, A. (2017b). Retinoic acid signaling maintains epithelial and mesenchymal progenitors in the developing mouse ureter. *Sci. Rep.* **7**, 14803. doi:10.1038/s41598-017-14790-2

Bohnenpoll, T., Wittern, A. B., Mamo, T. M., Weiss, A.-C., Rudat, C., Kleppa, M.-J., Schuster-Gossler, K., Wojahn, I., Ludtke, T. H.-W., Trowe, M.-O. et al. (2017c). A SHH-FOXF1-BMP4 signaling axis regulating growth and differentiation of epithelial and mesenchymal tissues in ureter development. *PLoS Genet.* **13**, e1006951. doi:10.1371/journal.pgen.1006951

Bussen, M., Petry, M., Schuster-Gossler, K., Leitges, M., Gossler, A. and Kispert, A. (2004). The T-box transcription factor Tbx18 maintains the separation of anterior and posterior somite compartments. *Genes Dev.* **18**, 1209-1221. doi:10.1101/gad.300104

Cao, M., Tasian, G., Wang, M.-H., Liu, B., Cunha, G. and Baskin, L. (2010). Urothelium-derived Sonic hedgehog promotes mesenchymal proliferation and induces bladder smooth muscle differentiation. *Differentiation* **79**, 244-250. doi:10.1016/j.diff.2010.02.002

Capone, V. P., Morello, W., Taroni, F. and Montini, G. (2017). Genetics of congenital anomalies of the kidney and urinary tract: the current state of play. *Int. J. Mol. Sci.* **18**, 796. doi:10.3390/ijms18040796

Cunha, G. R. (1976). Epithelial-stromal interactions in development of the urogenital system. *Int. Rev. Cytol.* **47**, 137-194. doi:10.1016/S0074-7696(08)60088-1

Firnberg, N. and Neubüser, A. (2002). FGF signaling regulates expression of Tbx2, Erm, Pea3, and Pax3 in the early nasal region. *Dev. Biol.* **247**, 237-250. doi:10.1006/dbio.2002.0696

Hafner, R., Bohnenpoll, T., Rudat, C., Schultheiss, T. M. and Kispert, A. (2015). Fgfr2 is required for the expansion of the early adrenocortical primordium. *Mol. Cell. Endocrinol.* **413**, 168-177. doi:10.1016/j.mce.2015.06.022

Hanafusa, H., Torii, S., Yasunaga, T. and Nishida, E. (2002). Sprouty1 and Sprouty2 provide a control mechanism for the Ras/MAPK signalling pathway. *Nat. Cell Biol.* **4**, 850-858. doi:10.1038/ncb867

Hoch, R. V. and Soriano, P. (2006). Context-specific requirements for Fgfr1 signaling through Frs2 and Frs3 during mouse development. *Development* **133**, 663-673. doi:10.1242/dev.02242

Hollnagel, A., Oehlmann, V., Heymer, J., Rüther, U. and Nordheim, A. (1999). Id genes are direct targets of bone morphogenetic protein induction in embryonic stem cells. *J. Biol. Chem.* **274**, 19838-19845. doi:10.1074/jbc.274.28.19838

Igarashi, M., Finch, P. W. and Aaronson, S. A. (1998). Characterization of recombinant human fibroblast growth factor (FGF)-10 reveals functional similarities with keratinocyte growth factor (FGF-7). *J. Biol. Chem.* **273**, 13230-13235. doi:10.1074/jbc.273.21.13230

Ikeda, Y., Zabbarova, I., Schaefer, C. M., Bushnell, D., De Groat, W. C., Kanai, A. and Bates, C. M. (2017). Fgfr2 is integral for bladder mesenchyme patterning and function. *Am. J. Physiol. Renal Physiol.* **312**, F607-F618. doi:10.1152/ajprenal.00463.2016

Jans, D. A. (1994). Nuclear signaling pathways for polypeptide ligands and their membrane receptors? *FASEB J.* **8**, 841-847. doi:10.1096/fasebj.8.11.8070633

Kurz, J., Weiss, A.-C., Thiesler, H., Qasrawi, F., Deuper, L., Kaur, J., Rudat, C., Lüdtke, T. H., Wojahn, I., Hildebrandt, H. et al. (2022). Notch signaling is a novel regulator of visceral smooth muscle cell differentiation in the murine ureter. *Development* **149**, dev199735. doi:10.1242/dev.199735

Laestander, C. and Engström, W. (2014). Role of fibroblast growth factors in elicitation of cell responses. *Cell Prolif.* **47**, 3-11. doi:10.1111/cpr.12084

Li, X.-J., Hu, B.-Y., Jones, S. A., Zhang, Y.-S., LaVaute, T., Du, Z.-W. and Zhang, S.-C. (2008). Directed differentiation of ventral spinal progenitors and motor neurons from human embryonic stem cells by small molecules. *Stem Cells* **26**, 886-893. doi:10.1634/stemcells.2007-0620

Liu, K. J. and Harland, R. M. (2003). Cloning and characterization of Xenopus Id4 reveals differing roles for Id genes. *Dev. Biol.* **264**, 339-351. doi:10.1016/j.ydbio.2003.08.017

Liu, Y., Jiang, H., Crawford, H. C. and Hogan, B. L. M. (2003). Role for ETS domain transcription factors Pea3/Erm in mouse lung development. *Dev. Biol.* **261**, 10-24. doi:10.1016/S0012-1606(03)00359-2

Mamo, T. M., Wittern, A. B., Kleppa, M.-J., Bohnenpoll, T., Weiss, A.-C. and Kispert, A. (2017). BMP4 uses several different effector pathways to regulate proliferation and differentiation in the epithelial and mesenchymal tissue compartments of the developing mouse ureter. *Hum. Mol. Genet.* **26**, 3553-3563. doi:10.1093/hmg/ddx242

Meuser, M., Deuper, L., Rudat, C., Aydoğdu, N., Thiesler, H., Zarnovican, P., Hildebrandt, H., Trowe, M.-O. and Kispert, A. (2022). FGFR2 signaling enhances the SHH-BMP4 signaling axis in early ureter development. *Development* **149**, dev200021. doi:10.1242/dev.200021

Moorman, A. F. M., Houweling, A. C., de Boer, P. A. J. and Christoffels, V. M. (2001). Sensitive nonradioactive detection of mRNA in tissue sections: novel application of the whole-mount in situ hybridization protocol. *J. Histochem. Cytochem.* **49**, 1-8. doi:10.1177/002215540104900101

Ornitz, D. M. and Itoh, N. (2015). The Fibroblast Growth Factor signaling pathway. *Wiley Interdiscip. Rev. Dev. Biol.* **4**, 215-266. doi:10.1002/wdev.176

Schindelin, J., Arganda-Carreras, I., Frise, E., Kaynig, V., Longair, M., Pietzsch, T., Preibisch, S., Rueden, C., Saalfeld, S., Schmid, B. et al. (2012). Fiji: an open-source platform for biological-image analysis. *Nat. Methods* **9**, 676-682. doi:10.1038/nmeth.2019

Shiroyanagi, Y., Liu, B., Cao, M., Agras, K., Li, J., Hsieh, M. H., Willingham, E. J. and Baskin, L. S. (2007). Urothelial sonic hedgehog signaling plays an important role in bladder smooth muscle formation. *Differentiation* **75**, 968-977. doi:10.1111/j.1432-0436.2007.00187.x

Tash, J. A., David, S. G., Vaughan, E. E. and Herzlinger, D. A. (2001). Fibroblast growth factor-7 regulates stratification of the bladder urothelium. *J. Urol.* **166**, 2536-2541. doi:10.1016/S0022-5347(05)65630-3

Trowe, M.-O., Maier, H., Petry, M., Schweizer, M., Schuster-Gossler, K. and Kispert, A. (2011). Impaired stria vascularis integrity upon loss of E-cadherin in basal cells. *Dev. Biol.* **359**, 95-107. doi:10.1016/j.ydbio.2011.08.030

Trowe, M.-O., Airik, R., Weiss, A.-C., Farin, H. F., Foik, A. B., Bettenhausen, E., Schuster-Gossler, K., Taketo, M. M. and Kispert, A. (2012). Canonical Wnt signaling regulates smooth muscle precursor development in the mouse ureter. *Development* **139**, 3099-3108. doi:10.1242/dev.077388

Velardo, J. T. (1981). Histology of the ureter. In *The Ureter* (ed. H. Bergman), pp. 13-54. New York: Springer-Verlag.
Walker, K. A., Sims-Lucas, S. and Bates, C. M. (2016). Fibroblast growth factor receptor signaling in kidney and lower urinary tract development. *Pediatr. Nephrol.* **31**, 885-895. doi:10.1007/s00467-015-3151-1
Wang, D.-Z. and Olson, E. N. (2004). Control of smooth muscle development by the myocardin family of transcriptional coactivators. *Curr. Opin. Genet. Dev.* **14**, 558-566. doi:10.1016/j.gde.2004.08.003
Wang, D.-Z., Chang, P. S., Wang, Z., Sutherland, L., Richardson, J. A., Small, E., Krieg, P. A. and Olson, E. N. (2001). Activation of cardiac gene expression by myocardin, a transcriptional cofactor for serum response factor. *Cell* **105**, 851-862. doi:10.1016/S0092-8674(01)00404-4
Weiss, A. C., Bohnenpoll, T., Kurz, J., Blank, P., Airik, R., Lüdtke, T. H., Kleppa, M. J., Deuper, L., Kaiser, M., Mamo, T. M. et al. (2019). Delayed onset of smooth muscle cell differentiation leads to hydroureter formation in mice with conditional loss of the zinc finger transcription factor gene Gata2 in the ureteric mesenchyme. *J. Pathol.* **248**, 452-463. doi:10.1002/path.5270
Yu, J., Carroll, T. J. and McMahon, A. P. (2002). Sonic hedgehog regulates proliferation and differentiation of mesenchymal cells in the mouse metanephric kidney. *Development* **129**, 5301-5312. doi:10.1242/dev.129.22.5301
Yu, K., Xu, J., Liu, Z., Sosic, D., Shao, J., Olson, E. N., Towler, D. A. and Ornitz, D. M. (2003). Conditional inactivation of FGF receptor 2 reveals an essential role for FGF signaling in the regulation of osteoblast function and bone growth. *Development* **130**, 3063-3074. doi:10.1242/dev.00491
Yu, Z., Mannik, J., Soto, A., Lin, K. K. and Andersen, B. (2009). The epidermal differentiation-associated Grainyhead gene Get1/Grhl3 also regulates urothelial differentiation. *EMBO J.* **28**, 1890-1903. doi:10.1038/emboj.2009.142
Zimmerman, L. B., De Jesús-Escobar, J. M. and Harland, R. M. (1996). The Spemann organizer signal noggin binds and inactivates bone morphogenetic protein 4. *Cell* **86**, 599-606. doi:10.1016/S0092-8674(00)80133-6

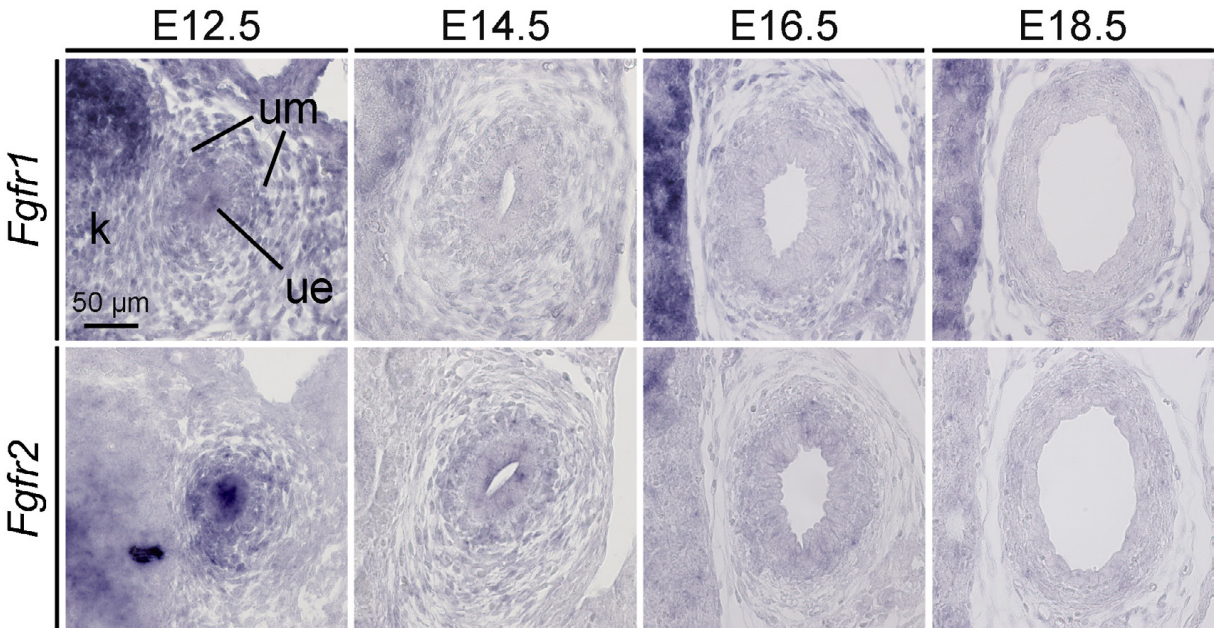

Fig. S1. *Fgfr1* and *Fgfr2* are expressed in the mesenchymal compartment of the developing ureter. RNA *in situ* hybridization analysis of *Fgfr1* and *Fgfr2* expression on transverse sections of the proximal ureter of E12.5 and E14.5 embryos. *n*=3 for each marker and stage. k, kidney; ue, ureteric epithelium; um, ureteric mesenchyme.

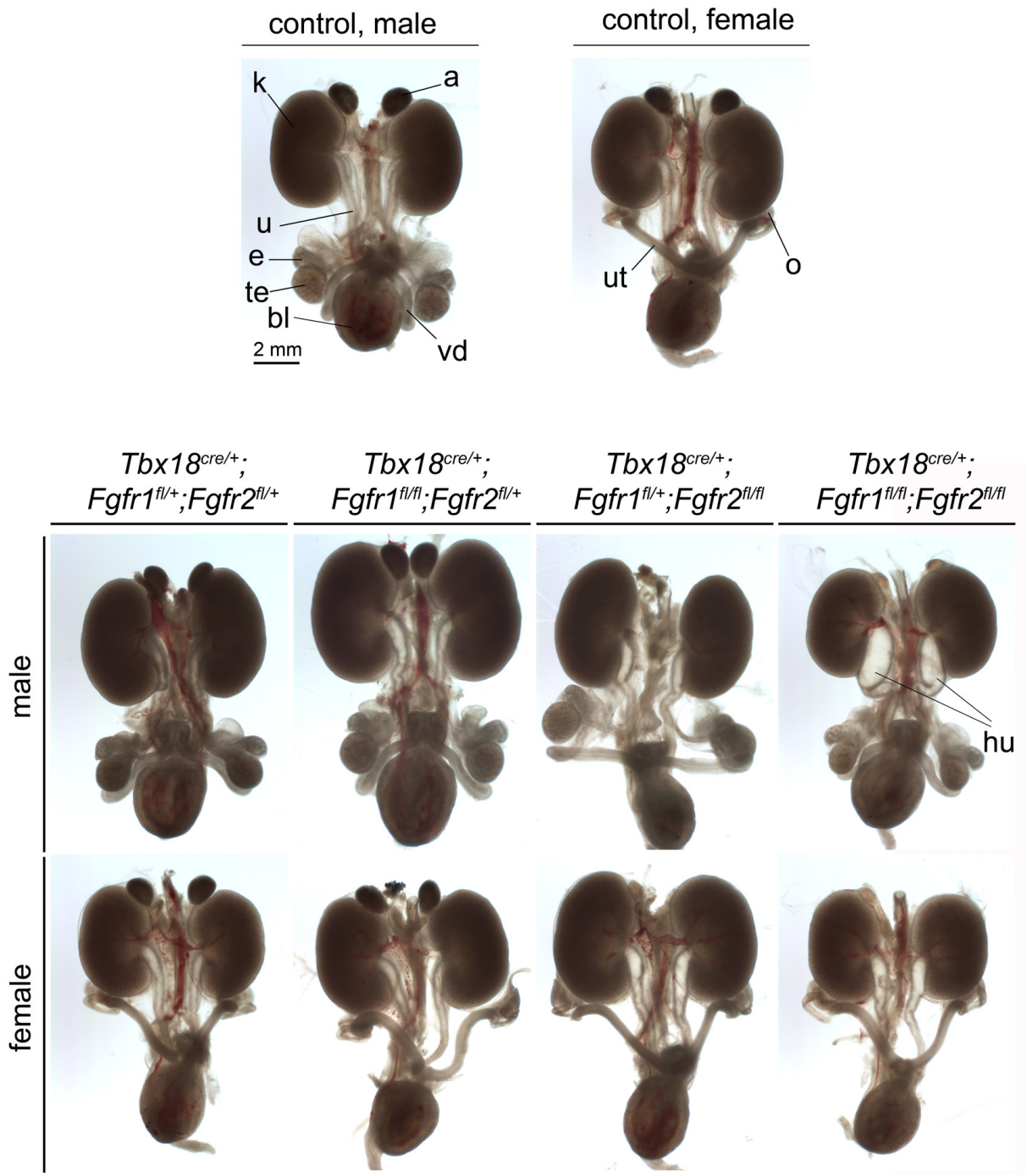

Fig. S2. Phenotypic variation of hydroureter formation upon loss of one or two alleles of *Fgfr1* and/or *Fgfr2* in the UM. Morphology of whole urogenital systems of male and female embryos at E18.5. Genotypes and sex are as indicated. For numbers see Table S2. a, adrenal; bl, bladder; e, epididymis; hu, hydroureter; k, kidney; o, ovary; te, testis; u, ureter; ut, uterus; vd, vas deferens.

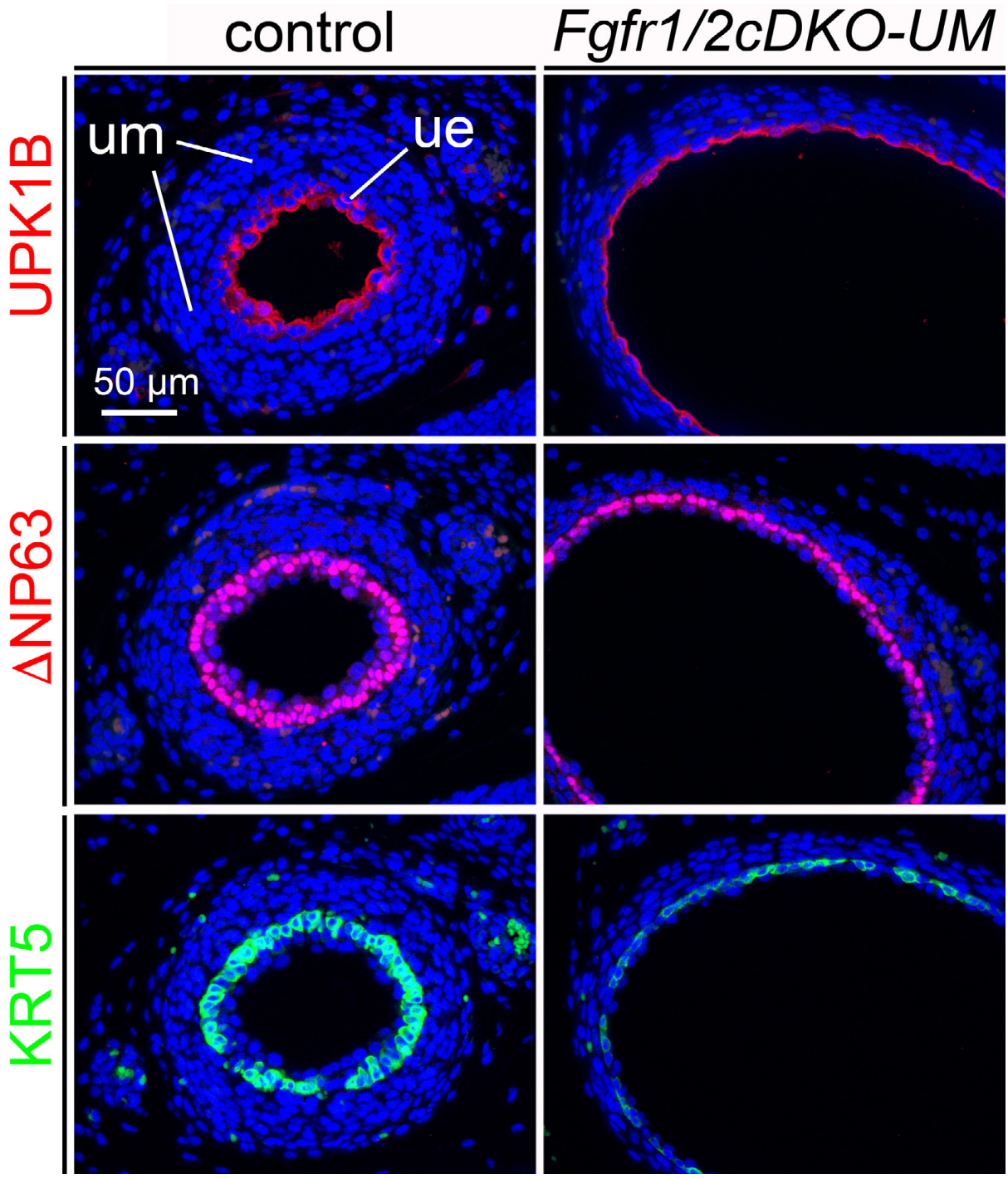

Fig. S3. Urothelial differentiation is not affected in *Fgfr1/2cDKO-UM* ureters at E18.5. Immunofluorescence analysis of expression of the urothelial marker proteins UPK1B (cytoplasmatic and extracellular, for superficial cells), ΔNP63 (nuclear, for intermediate and basal cells) and KRT5 (cytoplasmatic, for basal cells) on transverse sections of the proximal ureter of control and *Fgfr1/2cDKO-UM* embryos at E18.5. Nuclei are counterstained (in blue) with DAPI. Genotypes and antibodies are as indicated. $n \geq 3$ for each marker and genotype. ue, ureteric epithelium; um, ureteric mesenchyme.

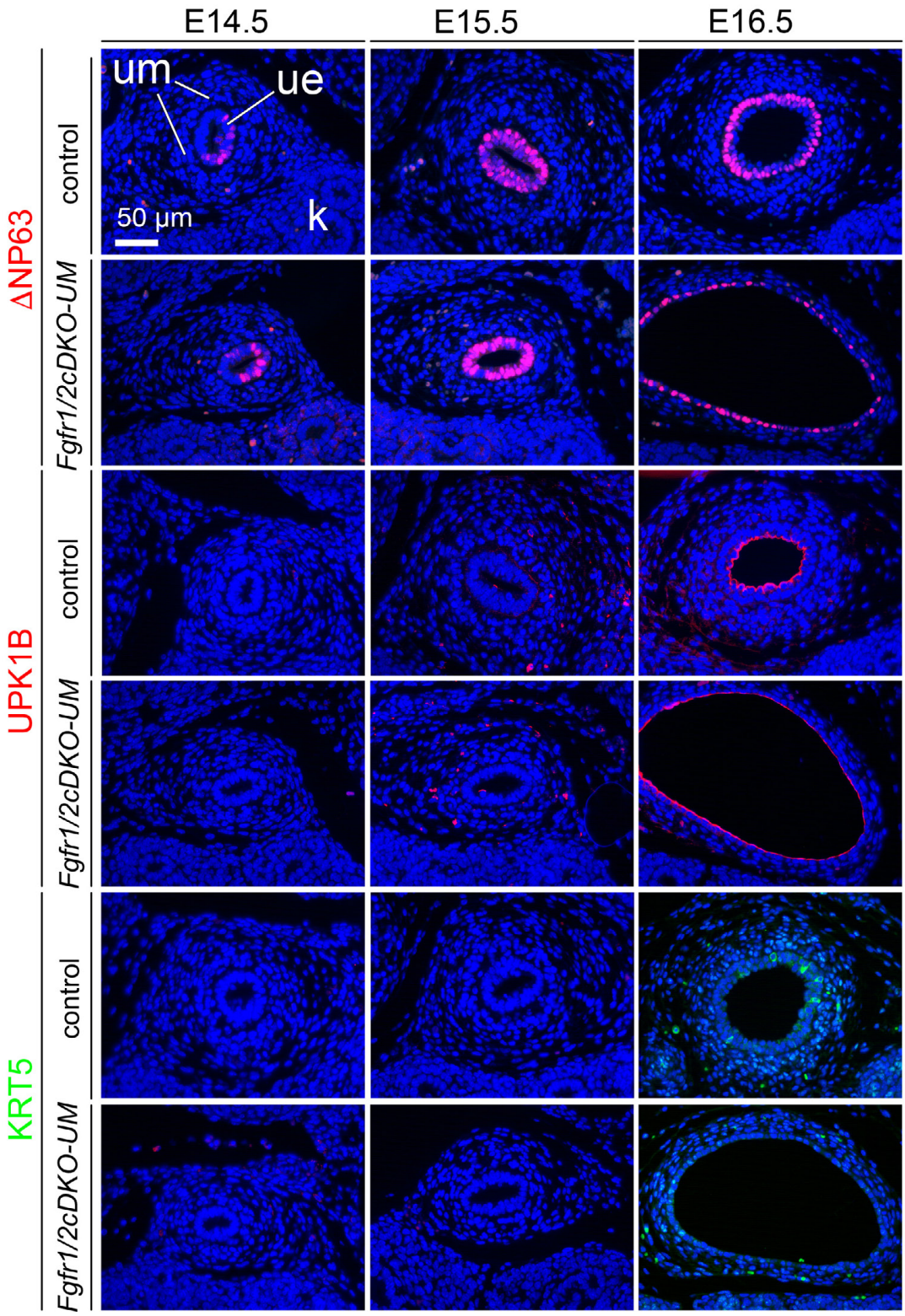

Fig. S4. Onset and progression of urothelial differentiation is not affected in *Fgfr1/2cDKO-UM* ureters at E14.5 to E16.5. Immunofluorescence analysis of expression of the urothelial marker proteins UPK1B (cytoplasmatic and extracellular, for superficial cells), ΔNP63 (nuclear, for intermediate and basal cells) and KRT5 (cytoplasmatic, for basal cells) on transverse sections of the proximal ureter of control and *Fgfr1/2cDKO-UM* embryos at E14.5, E15.5 and E16.5. Nuclei are counterstained (in blue) with DAPI. Genotypes and antibodies are as indicated. $n \geq 3$ for each marker, stage and genotype. k, kidney; ue, ureteric epithelium; um, ureteric mesenchyme.

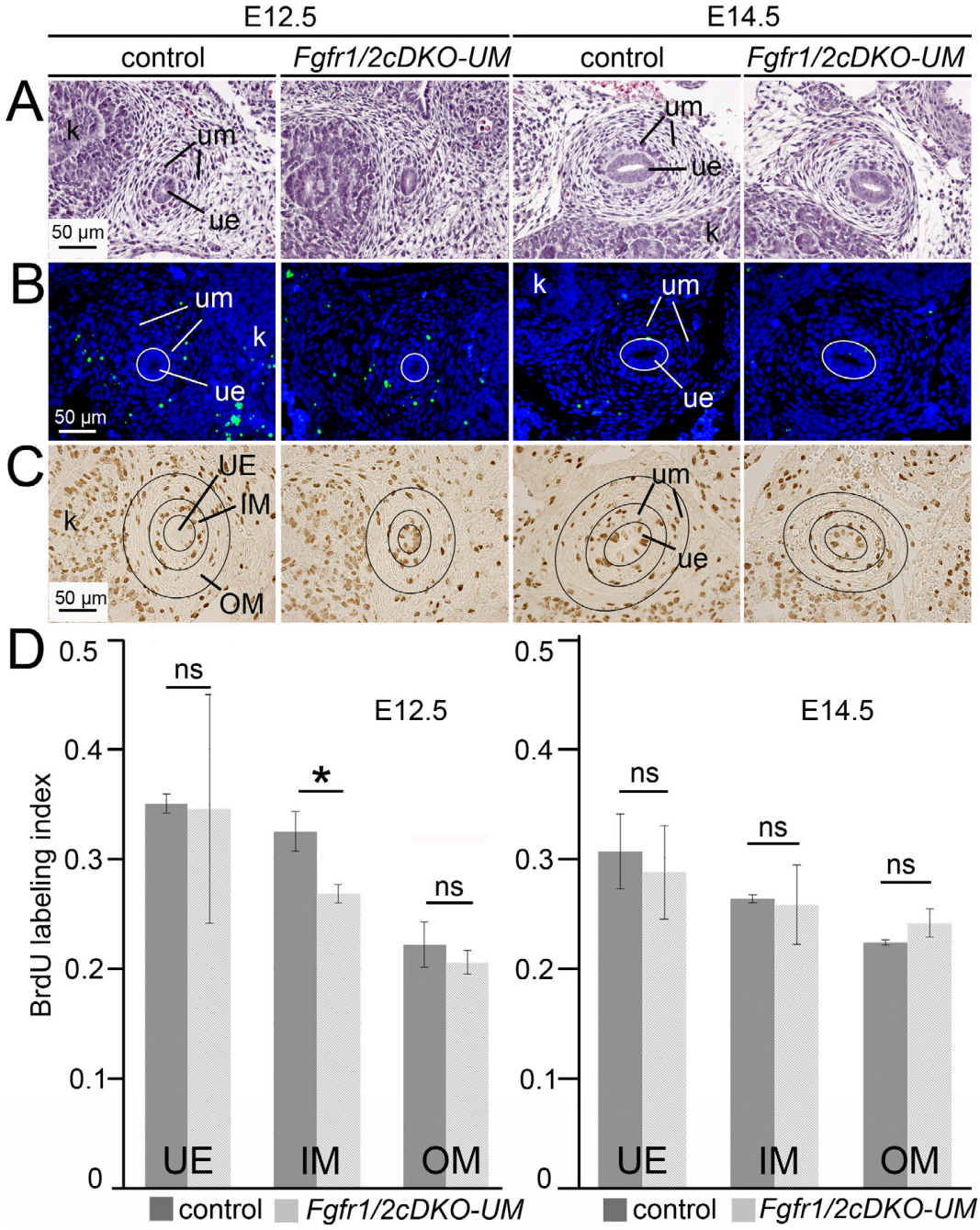

Fig. S5. *Fgfr1/2cDKO-UM* ureters exhibit reduced proliferation in the inner layer of the UM at E12.5. (A) Haematoxylin and eosin staining of transverse sections of the proximal ureter of control and *Fgfr1/2cDKO-UM* embryos at E12.5 and E14.5. (B) Immunofluorescence analysis (green) of apoptosis by the TUNEL assay on proximal ureter sections of control and *Fgfr1/2cDKO-UM* embryos at E12.5 and E14.5. Nuclei are counter-stained with DAPI (blue). $n \geq 3$ for each assay, stage and genotype. The white line indicates the ureteric epithelium. (C) Determination of cellular proliferation by the BrdU incorporation assay on transverse sections of the proximal ureter of control and *Fgfr1/2cDKO-UM* embryos at E12.5 and E14.5. Black circles mark the epithelium (UE) and the inner (IM) and outer (OM) mesenchymal compartments of the ureter in which proliferation was quantified (D). Quantification of BrdU-positive cells. Values are displayed as mean±sd. *, $P<0.05$; two-tailed Student's t-test. For detailed values see Table S3. k, kidney; ue, ureteric epithelium; um, ureteric mesenchyme.

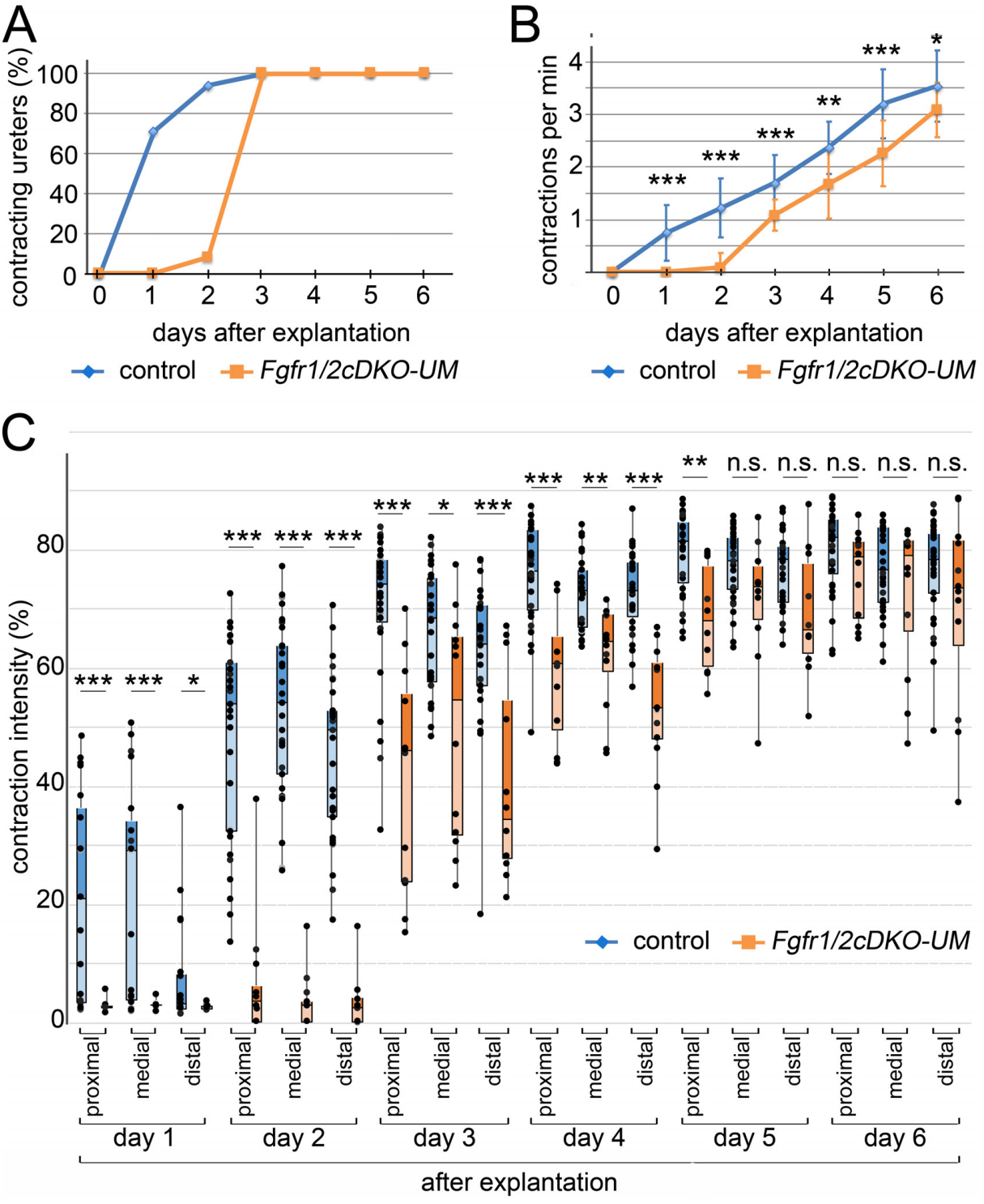

Fig. S6. Peristaltic activity in *Fgfr1/2cDKO-UM* ureters is delayed and reduced but not abrogated. (A-C) E15.5 ureters (control, *n*=32; *Fgfr1/2cDKO-UM, n*=12) were explanted and peristaltic activity observed for 6 days in culture. (A) Diagram showing the percentage of contracting ureters at any time-point of the culture. (B) Diagram of the contraction frequency (per min). (C) Box blot visualizing the contraction intensity. Statistical values are shown as mean±sd. *, P<0.05; **, P<0.01; ***, P<0.001; two-tailed Student's t-test. For detailed values see Table S5.

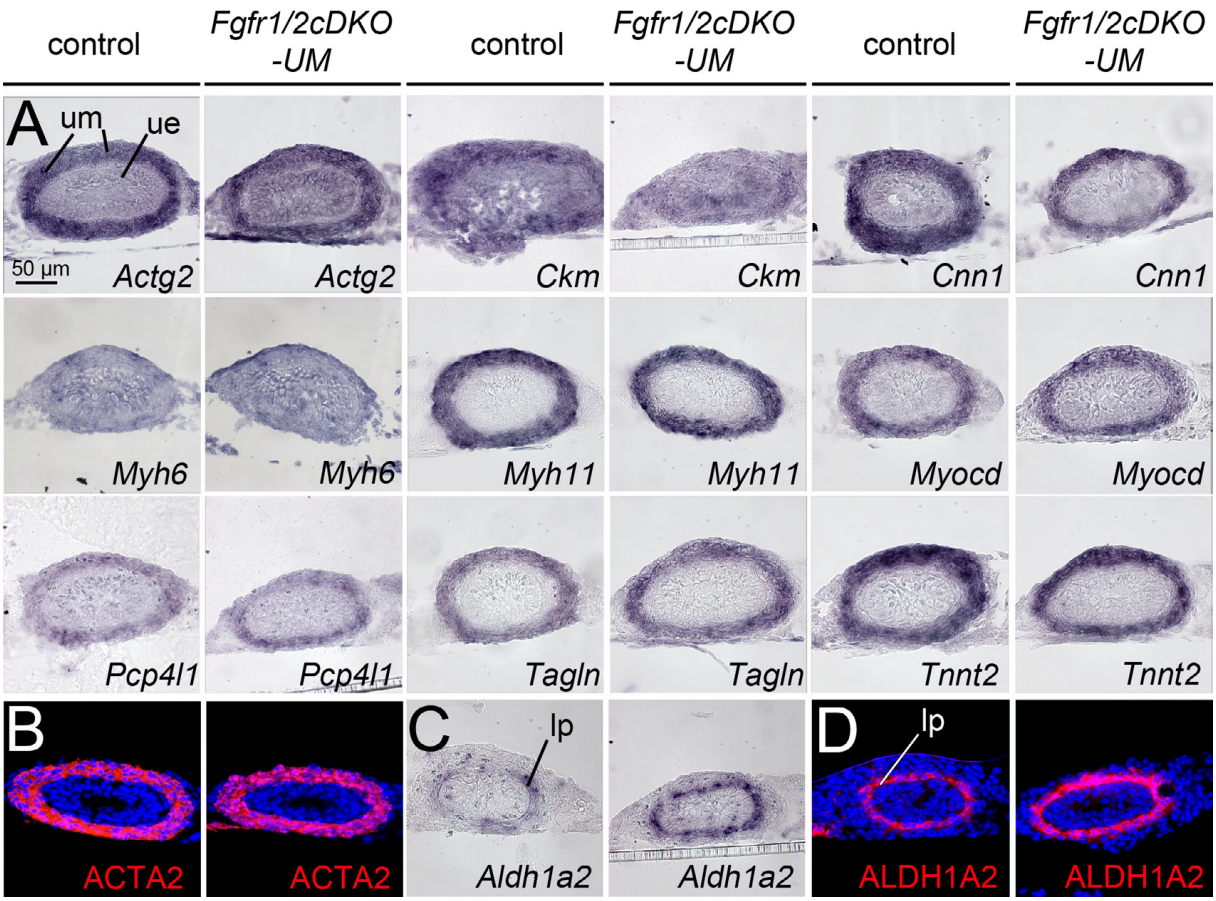

Fig. S7. SMC markers are largely unchanged in 6-day cultures of E15.5 *Fgfr1/2cDKO-UM* ureters. (A-D) Expression analysis on transverse sections of E15.5 ureter explants cultured for 6 days by RNA *in situ* hybridization (A,C) and by immunofluorescence (B,D) for SMC markers (A,B) and the *lamina propria* marker *Aldh1a2*/ALDH1A2 (C,D). *n*≥3 for each marker, assay and genotype. lp, lamina propria; ue, ureteric epithelium; um, ureteric mesenchyme.

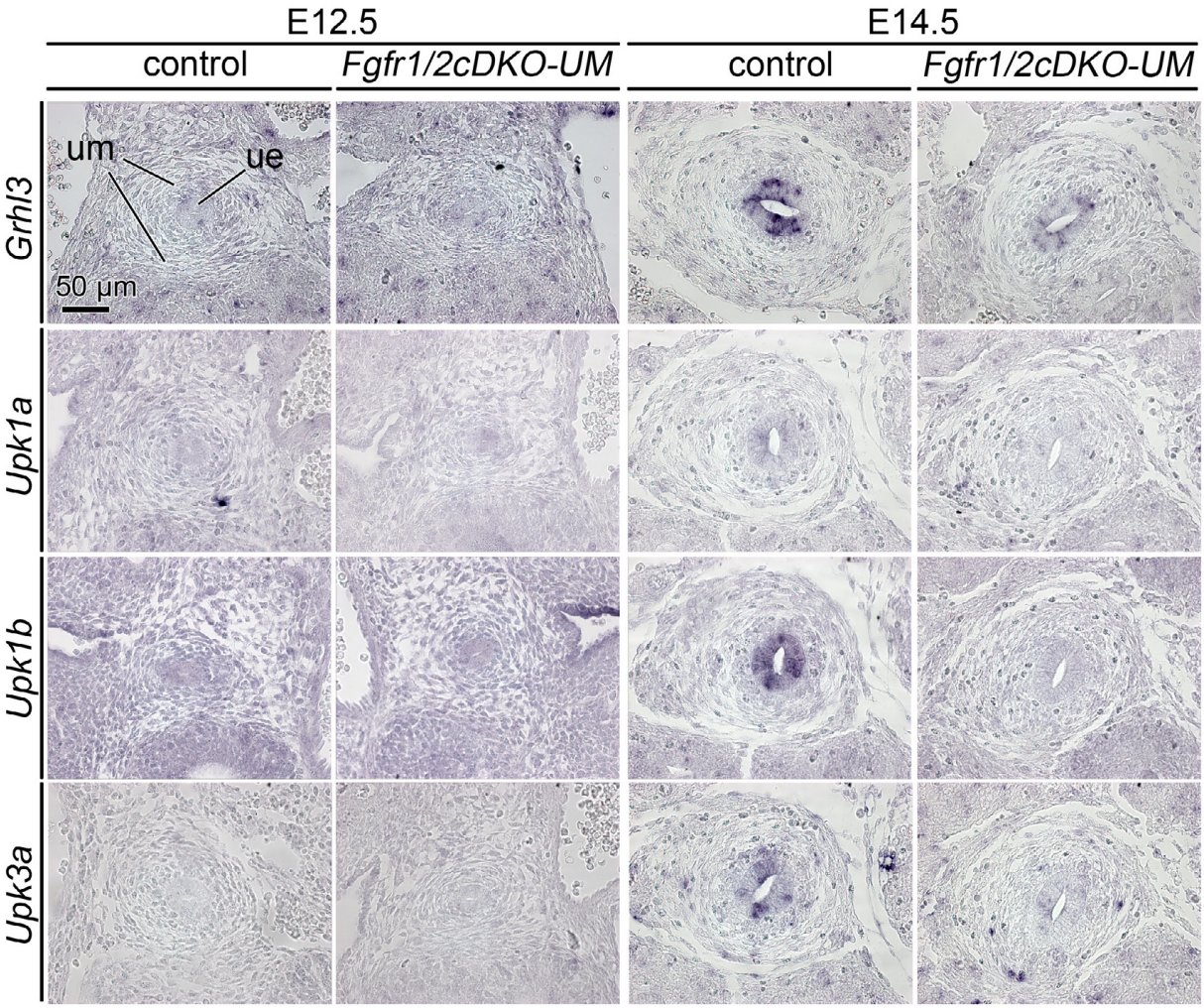

Fig. S8. Markers of superficial cells exhibit reduced expression in *Fgfr1/2cDKO-UM* ureters at E14.5. RNA *in situ* hybridization analysis on transverse sections of E12.5 and E14.5 ureters for expression of *Grhl3*, *Upk1a, Upk1b* and *Upk3a*. *n*≥3 for each probe, stage and genotype. ue, ureteric epithelium; um, ureteric mesenchyme.

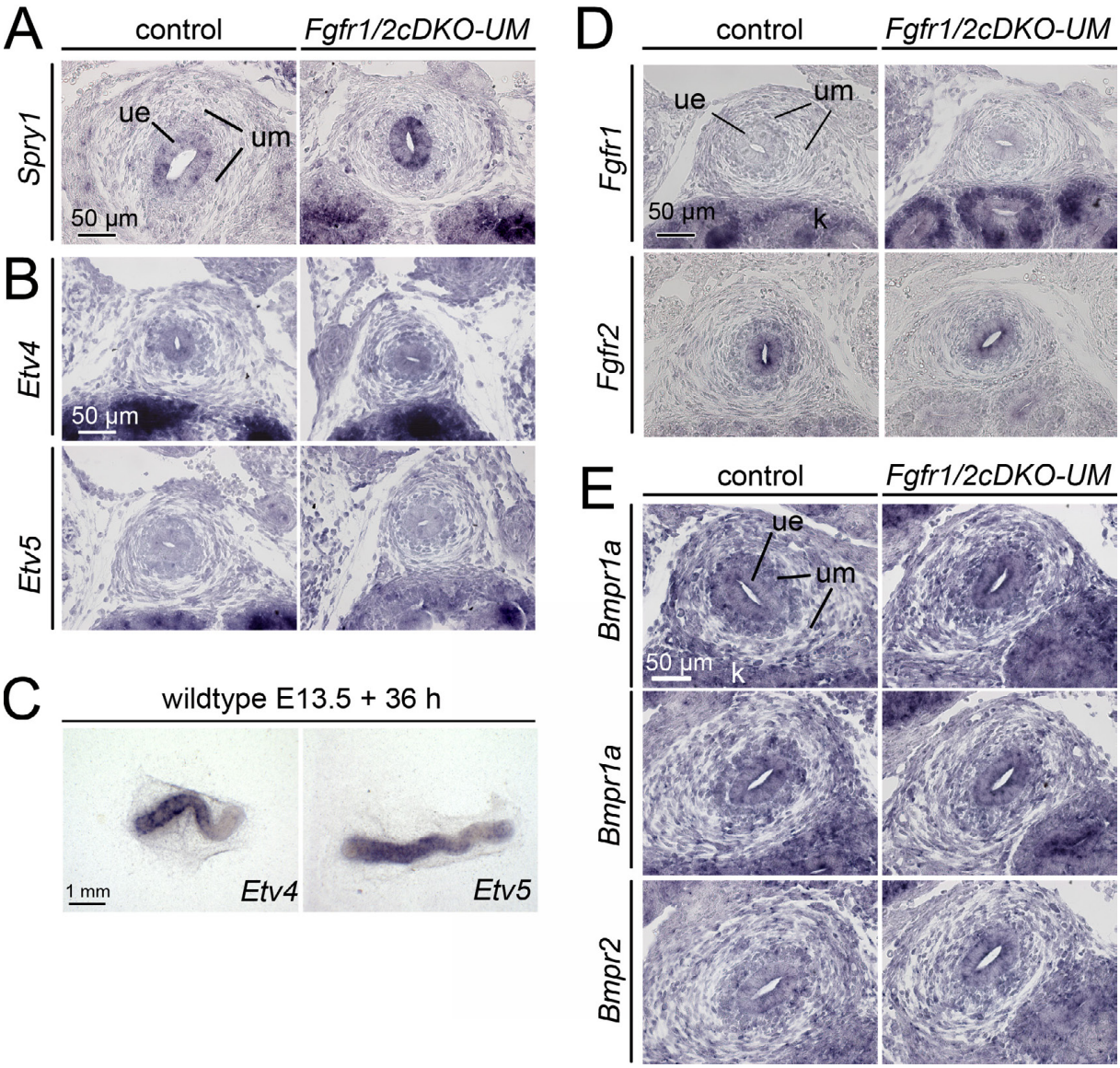

Fig. S9. Loss of mesenchymal *Fgfr1* and *Fgfr2* expression leads to increased epithelial FGFR2 signaling. (A-E) RNA *in situ* hybridization analysis of expression of *Spry1* (A), *Etv4* and *Etv5* (B,C), *Fgfr1* and *Fgfr2* (D) as well as *Bmpr1a*, *Bmpr1b* and *Bmpr2* (E) on transverse sections of the proximal ureter of *Fgfr1/2cKO-UM* and control embryos at E14.5 (A,B,D,E), and on whole E13.5 wild-type ureters cultured for 36 h (C). $n \geq 3$ for each probe and genotype. k, kidney; ue, ureteric epithelium; um, ureteric mesenchyme.

Table S1. Genotype distribution of embryos obtained from matings of *Tbx18*$^{cre/+;}$*Fgfr1*$^{fl/+;}$ *Fgfr2*$^{fl/+}$ males with *Fgfr1*$^{fl/fl}$;*Fgfr2*$^{fl/fl}$ females at E12.5, E14.5, E16.5 and E18.5.

Click here to download Table S1

Table S2. Distribution of hydroureter formation in urogenital systems of embryos obtained from matings of *Tbx18*$^{cre/+;}$*Fgfr1*$^{fl/+}$;*Fgfr2*$^{fl/+}$ males with *Fgfr1*$^{fl/fl}$;*Fgfr2*$^{fl/fl}$ females at E18.5.

Click here to download Table S2

Table S3. Quantification of the BrdU incorporation assay of proximal sections of control and *Fgfr1/2cDKO-UM* embryos at E12.5 and E14.5.

Click here to download Table S3

Table S4. Statistics on the peristaltic activity of explants of E13.5 *Fgfr1/2cDKO-UM* ureters cultured for 6 days.

Click here to download Table S4

Table S5. Statistics on the peristaltic activity of explants of E15.5 *Fgfr1/2cDKO-UM* ureters cultured for 6 days.

Click here to download Table S5

Table S6. List of genes with increased expression in the microarray of E15.5 ureters of *Fgfr1/2cDKO-UM* and control embryos cultured for 6 days.

Click here to download Table S6

Table S7. List of genes with decreased expression in the microarray of E15.5 ureters of *Fgfr1/2cDKO-UM* and control embryos cultured for 6 days.

Click here to download Table S7

Table S8. Functional annotation by DAVID for genes with increased expression in the microarray of E15.5 *Fgfr1/2cDKO-UM* ureter explants cultured for 6 days.

Click here to download Table S8

Table S9. Functional annotation by DAVID for genes with decreased expression in the microarray of E15.5 *Fgfr1/2cDKO-UM* ureter explants cultured for 6 days.

Click here to download Table S9

Table S10. List of genes with decreased expression in the microarray of E14.5 ureters of *Fgfr1/2cDKO-UM* and control embryos.

Click here to download Table S10

Table S11. List of genes with increased expression in the microarray of E14.5 ureters of *Fgfr1/2cDKO-UM* and control embryos.

Click here to download Table S11

Table S12. Functional annotation clustering by DAVID for genes with decreased expression in the microarray of E14.5 *Fgfr1/2cDKO-UM* ureters.

Click here to download Table S12

Table S13. Functional annotation clustering by DAVID for genes with increased expression in the microarray of E14.5 *Fgfr1/2cDKO-UM* ureters.

Click here to download Table S13

Table S14. Expression analyses by RT-qPCR analysis.

Click here to download Table S14

Table S15. Genes with decreased expression in microarrays of E13.5 *Pax2cre/; Fgfr1*$^{fl/+}$*;Fgfr2*$^{fl/fl}$ *(Fgfr1/2cDKO-UE)* ureters.

Click here to download Table S15

Table S16. Statistical analysis of contraction frequencies of explants of E13.5 ureters cultured for 8 days in the presence of purmorphamine and/or NOGGIN.

Click here to download Table S16

Table S17. Primers for qRT-PCR analysis of gene expression.

Click here to download Table S17